ELECTROMAGNETIC FIELDS INDUCED IN A SOLID CYLINDRICAL VOLUME CONDUCTOR DUE TO SWITCHING OF MRI Z GRADIENT FIELD: APPLICATION TO PERIPHERAL NERVE STIMULATION

By

Getachew Debela Mamo

ADDIS ABABA UNIVERSITY
PROGRAM OF GRADUATE STUDIES
DEPARTMENT OF PHYSICS

A Thesis/Project Submitted to the Graduate Program of Addis Ababa University in Partial Fulfilment of the Requirements for the Degree of Master of Science in Physics (Imaging Physics)

Advisor

Dr. Tesfaye Kidane

ADDIS ABABA UNIVERSITY

PROGRAM OF GRADUATE STUDIES

DEPARTMENT OF PHYSICS

STATEMENT OF THESIS/PROJECT APPROVAL

The under-signed, **Members of the Examining Committee**, hereby certify that they have read and recommended to the Department of Physics for acceptance of this thesis/project entitled **"ELECTROMAGNETC FIELDS INDUCED IN A SOLID CYLINDRICAL VOLUME CONDUCTOR DUE TO SWITCHING OF MRI Z GRADIENT FIELD: APPLICATION TO PERIPHERAL NERVE STIMULATION"** by **Getachew Debela Mamo** in partial fulfillment of the requirements for the degree of **Master of Science in Physics (Imaging Physics).**

ADVISOR: Dr. Tesfaye Kidane

Signature _____

EXAMINOR: Professor A.V.Gholap

Signature _____

EXAMINOR: Dr. Teshome Senbeta

Signature _____

CHAIRMAN: Dr. Chernet Amente

Signature _____

June 18 2018, Addis Ababa

Ethiopia

ADDIS ABABA UNIVERSITY

PROGRAM OF GRADUATE STUDIES

DEPARTMENT OF PHYSICS

STATEMENT OF AUTHOR DECLARATION

AUTHOR:- Getachew Debela Mamo

TITLE:- ELECTROMAGNETIC FIELDS INDUCED INSIDE A SOLID CYLINDRICAL VOLUME CONDUCTOR DUE TO SWITCHING OF MRI Z GRADIENT FIELD: APPLICATION TO PERIPHERAL NERVE STIMULATION

DEPARTMENT:- PHYSICS

DEGREE:- M.SC. **CONVOCATION:-** JUNE 2018

PERMISSION IS HERE GRANTED TO ADDIS ABABA UNIVERSITY TO CIRCULATE AND TO COPY FOR NON COMMERCIAL PURPOSE, AT ITS DISCRETION, THE ABOVE TITLE, UPON THE REQUEST OF INDIVIDUALS AND INSTITUTIONS.

Signature of the Author

THE AUTHOR DOES NOT RESERVE OTHER PUBLICATION RIGHTS, NEITHER THE THESIS/PROJECT NOR EXTENSIVE EXTRACTS FROM IT, MAY BE PRINTED OR OTHERWISE REPRODUCED WITHOUT THE AUTHOR'S WRITTEN PERMISSION

THE AUTHOR ATTESTS THAT FOR ALL USE OF ANY COPYRIGHTED MATERIALS APPEARING IN THIS THESIS/PROJECT, PROPER ACKNOWLEDGEMENT HAS BEEN MADE.

DEDICATION

In Loving Memory of my Mother - **FELEKECH DESTA**- the absolute emblem of love and care for me - on earth. Thank you so much **FELIE**, and I am still strong because of you. Thank you so much, for implanting in my mind, fairness and respect for people.

ACKNOWLEDGEMENTS

I am deeply indebted to my advisor Dr. Tesfaye Kidane for his unreserved professional advice, continuous follow up and support during the time of my study. His guidance and instruction methodology has enabled me to accomplish my task successfully and has instilled an inspiration for my future work, God willing.

My deeper gratitude goes to Dr. Mulugeta Bekele - my undergraduate wonderful instructor 28 years ago, who has become a cause to learn this very fascinating science of imaging physics. He has created a new career opportunity and has given me a reason for enjoying lifelong professional pleasure.

I would like to thank my graduate instructors - Professor A.K. Chaubey, Dr. Teshome Senbeta, Dr. Belayneh Mesfin, Dr. Derbie Hirpo, Dr. Tatek Yergou and Mr. Lemma Setegn (Pedagogic), for sharing their knowledge to me, and as I perceive it, for being a cause for a wonderful and unforgettable sweet experience in my life.

My appreciation goes to the Ministry of Education for sponsoring me to pursue a master's degree education and my working department - National Mathematics and Science Education Improvement Center, for its support to me while I was studying. I also appreciate the department of physics of Addis Ababa University for providing the necessary learning resources for my study.

I thank all the members of my family and friends, for encouraging and supporting me as well as sharing all sorts of my feelings - pain and success.

Finally I express my deepest respect for researchers all over the globe, both alive and otherwise, who strove day and night in search of the objective scientific truth which resulted in the invention of helpful technologies for human race, and those whose writings I have been reading and referring to accomplish my study.

Getachew Debela Mamo

Addis Ababa

Ethiopia

June 18, 2018

TABLE OF CONTENTS

ABSTRACT

The rapid switching frequency of MRI gradient fields has a direct relationship to the resolution and hence to the quality of the image. Hence, there is a tendency in the research area to increase the frequency of switching even more. However, the rapid switching frequency can create unwanted peripheral nerve stimulation on the patient's body due to the eddy current induction. In this report a model of the induction of the magnetic and electric fields as well as the eddy current in a solid cylindrical volume conductor (human body model) due to the switching of the Z gradient coils have been explored analytically. The coils are assumed to carry time harmonic variable current at low frequency. For the analysis, Maxwell's Equations are approximated for this quasi-static situation. Starting from the vector potential expression and taking the first order asymptotic approximations of the modified Bessel functions, the solutions for the field vectors and the eddy current expression in the cylinder have been found. The application of the problem to peripheral nerve stimulation and the mechanism of PNS in the aspect of its useful application has been discussed. The plot of the eddy current density against the radial distance in the cylinder has shown that the peripheral nerve stimulation is confined to the peripheral surface of the patient's body. The solutions have important implication in the design of MRI gradient coils to avoid PNS during scanning and ensure patient safety and comfort.

LIST OF FIGURES

LIST OF ABBREVIATIONS

RF	Radio Frequency
FT	Fourier Transform
MR	Magnetic Resonance
CT	Computed Tomography
GE	General Electric
FE	Finite Element
FD	Finite Difference
PC	Personal Computer
MS	Multiple Sclerosis
NMR	Nuclear Magnetic Resonance
MRI	Magnetic Resonance Imaging
EMF	Electromagnetic Field
FID	Free Induction Decay
MHz	Megahertz
IFT	Inverse Fourier Transform
CNS	Central Nervous System
SNR	Signal-to-Noise Ratio
CNR	Contrast-to-Noise Ratio
TMS	Transcranial Magnetic Stimulation
MEG	Magnetoencephalography
PNS	Peripheral Nerve Stimulatiton
ODE	Ordinary Differential Equation
SAR	Specific Absorption Rate
OCT	Optical Coherence Tomography
SQUID	Superconducting Quantum Interference Device

CHAPTER 1
INTRODUCTION TO MAGNETIC RESONANCE IMAGING

1.1 Magnetic Resonance Imaging

Magnetic resonance imaging (MRI) is a technique of getting an image of the inside part of the human body with out having to do operation, but instead by using the phenomenon of nuclear magnetic resonance (NMR). The NMR phenomenon is a phenomenon where, if nuclei are kept in a magnetic field, they can absorb incoming EM energy sent towards them from outside, and then emit the EM energy later during the time the nuclei relax. Nowadays this imaging modality is offering great promise in understanding much more about the human body both in its shape and function [1].

The NMR phenomenon was first discovered by Isidor Isaac Rabi, while he was trying to record the magnetic properties of some atomic nuclei. For this work he was awarded the 1944 Nobel Prize in physics. Later on the physicists Flex Bloch and Edward Purcell detected the same NMR phenomenon in water and in paraffin respectively. They demonstrated the NMR phenomenon independently in 1946. In addition the two scientists developed a new method for nuclear magnetic precision measurement that works based on NMR. For this work they won the Noble price together in 1952.

When NMR was started to be used for imaging purpose in the 1970th, it was originally called NMRI (Nuclear Magnetic Resonance Imaging). However, the public at the time, did not have good feeling for the word *Nuclear* and therefore the letter N had been dropped and hence is MRI [2]. Nevertheless, MRI is a purely nuclear origin and the NMR discovery is key to its functioning. MRI is called non-invasive[1] and pain free technique of imaging.

Another interesting feature of this technique is that there is no ionizing radiation used as in the case of X - ray or CT scans. In MRI a system of magnetic fields is employed for imaging. As a result, there is no any potential danger or side effect on the person, that comes from the sole magnetic fields, during and after MRI scan, as long as the relevant and proper procedure is strictly followed.

The image we get from MRI has a very high contrast for soft tissues such as the brain and the heart with a very high image resolution. And this is one of the several characteristic that makes MRI better than other imaging methods [3]. MRI is now being used widely in health centers in many parts of the world for diagnostic and research purposes as well as for monitoring treatments of the internal parts of the human body .

1.2 The Basic Working Principles of MRI

Elementary particles have been found to possess a fundamental quantum property called *spin* which gives them a magnetic property. Accordingly, the proton has

[1]Non-invasive means there is no surgery

a magnetic property and possesses a nuclear magnetic moment. Naturally in our body there are a lot of hydrogen protons contained in water molecules. This means each hydrogen proton in our body behaves like a tiny microscopic magnet with a magnetic dipole [4].

The fact that the proton has a magnetic moment was first discovered by the Stern and Gerlach experiment in 1922. That was a very vital discovery for MRI technology. The proton has a magnetic moment means, it can interact with any other external magnetic field or set of magnetic fields.

From the classical point of view, having spin is meant that the particle (proton) rotates (spins) about its own axis. In addition, since the proton carries an electric charge, as it spins, it acts like a tiny circular current, producing its own tiny magnetic field and acquiring a nuclear magnetic dipole moment $\vec{\mu}_p$ as stated earlier.

Suppose that there are several protons at a certain location in space. If these several protons are left alone without the presence of any strong external magnetic field, then each proton spins in any arbitrary direction as shown in Fig. 1.1 (a). And the total effect is that there will be no net magnetic moment (also called magnetization vector) because the sum of the spin vectors is zero as they cancel one another. In this case, since there is no *net magnetic moment* of the spins, we can not talk about MRI.

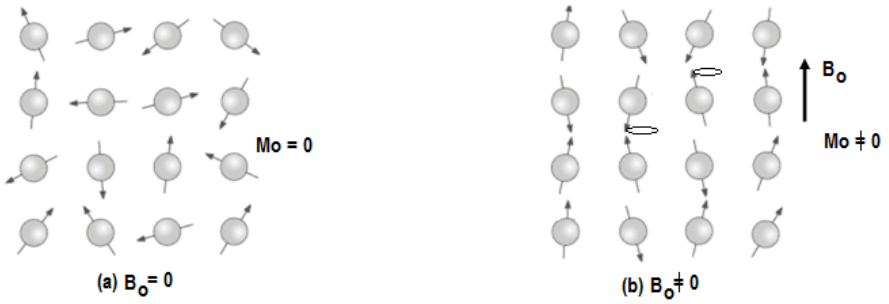

Figure 1.1: (a) Spins are randomly oriented in the absence of $\vec{B}_0$ and so $\vec{M}_0 = 0$ (b) Spins are aligned in the same or opposite to $\vec{B}_0$ direction and $\vec{M}_0 \neq 0$

However, if there exists an external magnetic field passing through the location where the spis are found, and which is strong enough to affect the spins, then the spins will align themselves along the external magnetic field $\vec{B}_0$, some of them in the same direction and others in the opposite direction to the field as shown in Fig. 1.1 (b). However, no one of the spins align 100% perfectly with the external static field because of the non-zero thermal energy each spin possesses. At thermal equilibrium, most nuclear spins exist in the lowest energy state and as the temperature increases the number of spins which will be in the higher energy state will increase [5].

Out of the total number of the spins that are found in the external magnetic field, the distribution of the number of spins in the lower and upper energy states is governed by Boltzmann statistical distribution law which is given as

$$\frac{N_{high}}{N_{low}} = e^{-\frac{\Delta E}{kT}} \tag{1.1}$$

N_{high} is the number of spins in the high energy level (opposite to the main field)

and N_{low} is the number of spins in the low energy level (along the main field). ΔE is the energy difference between the two levels or states, k is Boltzmann constant and T is the absolute temperature of the spins or the sample containing the spins.

The Boltzmann distribution expression above implies that those spins that align in the same direction as the external magnetic field (lower energy state) slightly outnumber the spins that are aligned in the opposite direction (higher energy state).

This means, there will always be a net (equilibrium) magnetic vector in the direction of the external magnetic field as long as the spins are found with in the external magnetic field. This net magnetic field is called equilibrium magnetization vector and is symbolized by $\vec{M}_0$. The creation of this equilibrium magnetization vector $\vec{M}_0$ from the product of the excess spins number and the nuclear magnetic moment of a single spin in the sample is crucial for MRI.

The human body, which has abundant water, and hence ample hydrogen proton content, can be considered to be almost full of tiny magnets all randomly oriented with the net effect being zero, in the absence of an external strong magnetic field, and that is always true as you live your everyday life. In other words every person is not found in a strong magnetic field but only found in the magnetic field of the earth which is very weak in its magnitude and is approximated to be about 3.0×10^{-5} Tesla. And this earth's magnetic field does not affect the proton spins in a person's body and every person can be considered to have no net magnetization in his/hers body in every day to day life.

However, if we produce a much greater external strong and uniform magnetic field $\vec{B}_0$, for instance, as strong as 1.5 Tesla or more, and put a person inside the strong magnetic field, at this time, the tiny magnets (hydrogen protons) in the body of the person, originally randomly oriented, will align themselves some of them in the direction of the external field and others opposite to the external magnetic field direction. Consequently the person will be magnetized possessing a net magnetization vector $\vec{M}_0$.

The external field exerts magnetic force on each spinning proton which possesses tiny magnetic field . A magnetic force on a spinning proton having a nuclear magnetic dipole moment creates torque on the magnetic moment. As a result the torque makes each proton to go around the main magnetic field and this type of motion is called *precession*. The protons in the external magnetic field perform two types of motion. That is spinning around their own axis and also rotate (precess) around the external magnetic field direction at the same time - that is, some in the same direction as the main magnetic field and others in the opposite direction. Fig 1.1b.

As discussed before, there will be a net magnetic field (called a net magnetization vector) which will be generated in the person's body and is directed in the same direction as the external magnetic field. This magnetization is the sum of those excess spins or magnetic dipole moments.

With a person kept inside a strong magnetic field, and once the net magnetization is formed in his body, the next task is manipulation of this magnetization vector using a radio frequency (RF) field. The RF field is generated by a nearby coil and sent from outside towards the person perpendicular to $\vec{M}_0$. We send a pulse of RF field (RF field is another magnetic field - $\vec{B}_1$ which is of the order of milli-Tesla.) to the person who is placed inside the main external magnetic field.

The purpose of the RF field is to disturb the net magnetization vector created in the person's body from its stable equilibrium alignment along $\vec{B}_0$. When the RF field is off, the magnetization vector restores its equilibrium magnitude and original undisturbed position as it continues precession towards its initial orientation.

With a series of purposeful RF energy exposure - that is by a continuous RF pulses, the magnetization vector fluctuates in its magnitude and direction varying all the way from its maximum value to its minimum value and vice versa. This is the same as having a changing or a time varying magnetic field.

If there is a changing magnetization vector (changing magnetic field), then by bringing a coil of wire closer to the changing magnetization (that is closer to the person's body), a signal can be collected by the coil. Since the magnetization vector is equal to a changing magnetic field vector, magnetic flux variation will be created when the variable field crosses through the coil area.

By Faraday's law of EM induction, the magnetic flux change through the coil produces a potential difference or current in the coil. This potential difference or current is the very signal that carries the image information of the interior part of the person's body.

In this way, any part of the body can be imaged in any kind of orientation required. However, in order to choose the part of the body to be imaged as required, we need to add another kind of magnetic fields on to the main strong and uniform magnetic field, where the new magnetic fields create a slight and linear variation in the main field. These magnetic fields are called gradient fields. The gradient fields are created along the three axes - x, y and z (labled $\vec{G}_x$, $\vec{G}_y$ and $\vec{G}_z$). The x and y gradient fields are created by transverse gradient coils and the z gradient field is generated by longitudinal gradient coil.

The slight variation in the main field due to the gradient fields at different parts of the body will create different frequency of precession of the magnetization at any point or location (from head to toe) in the body. And that enables us to choose any part of the body by using an RF field which has the same frequency as the spins or magnetization vector in the part of the body chosen for imaging.

The signal receiving coil collects a continuous or analog signal. Before the analog signal gives the required image of the person's body, it will be stored in a computer memory as a raw digital data. Then after several relevant and necessary mathematical techniques, such as sampling, digitization and other electronic and engineering procedures are done on the signal (this is called signal processing) before we get the image on the computer display screen. Then the image will be read and examined by a professional personnel for a subsequent clinical examination.

1.3 Major Components of MRI Machine

Starting from the generation of the magnetization vector in the person's body all the way to the formation of a final quality image on the computer screen, the MRI machine utilizes many hardware parts. However, the most important are the following ones.

1.3.1 The Main Magnet

The main magnet can be a very strong permanent magnet. Or it can be a magnet made from a current carrying superconducting coil or electromagnet. In the case of the electromagnet, the coil is mostly made from the compound Niobium-Titanium (NbTi). Niobium-Titanium is an alloy of the elements Niobium and Titanium with a critical temperature value of about 10 kelvin. It is mostly used as a superconducting wire to produce strong electromagnetic field. This wire will be kept in a cooling liquid such as Helium with a temperature as close as to the absolute zero.

At this low temperature the resistance of the coil will drop to zero and the coil will be a superconductor with zero resistance and be able to carry large current. Then allowing the right variable current value to pass through the coil will induce a very strong and homogeneous magnetic field.

The strong magnetic field which will be created by the large current is situated in a large cylindrical or any other appropriate opening designed to let the patient inside. This strong field is responsible for aligning all the proton spins in the person's body parallel to it and create a net longitudinal magnetization vector. Therefore, the main magnet is the back bone of the MRI machine that creates the net magnetization vector which is going to be manipulated frequently using an RF field to generate the image signal.

1.3.2 The Shim Coil

In order to get a clear image the main magnetic field strength has to be very uniform or homogeneous everywhere in the imaging volume or location [6]. However, practically the main magnetic field may have a very slight inhomogeneities that may be caused by several factors. The factors could be, such as for instance, imperfections in the process of designing the magnet and imperfections in winding and placing of the superconducting wires and the like.

Because of the presence of slight magnetic field non-uniformity or inhomogeneity in the main magnetic field, image distortion, image blurring and signal loss may occur. Hence as much as possible there should always be a means to minimize or avoid the main field inhomogeneity.

One way of eliminating the inhomogeneities is to add another coil called shimming coil which is designed to create small magnetic field such that it opposes or counteracts the inhomogeneity in the main field and helps to gain better homogeneous main field. This process is called shimming.

Shimming is the act of making the main magnet field more perfectly uniform by decreasing the inhomogeneities as much as possible to zero in the imaging volume. It is the process of adjusting the magnetic field to achieve the best possible homogeneity so that there will not be variation in the field strength from point to point in the imaging volume [7].

1.3.3 The Gradient Coils

Any point in the imaging volume in the main magnetic field is made spatially unique and frequency dependent through the application of the gradient fields as stated earlier. The gradient coils produce these secondary magnetic fields called

gradient fields which are additions of slight and linearly variable fields on the main field in all the three dimensions x, y and z [8].

The purpose of the gradient fields is to create a linear and controllable field variation on the static field $\vec{B}_0$ anywhere in the scanner or in the imaging volume. The gradient fields add and subtract some value from $\vec{B}_0$ when going outward from the origin in the positive and negative directions of the three axes. At a point called iso-center, that is at the middle of the imaging volume, the $\vec{B}_0$ has its original (unmodified) value.

Using the gradient field and creating a slight variation of the main magnetic field enables the proton spins to precess with different frequency at different parts of the body. This means a certain frequency of precession is associated to a specific spatial location in the body that can be identified easily for imaging.

But if there is no variation in frequency of precession of the spins, there will be only one kind of frequency by which all parts of the body precess, and we cannot identify from which part of the body has the signal originated and this means the specific imaged body part is not known.

The physical and technical concept of using small variable gradient fields along with the main uniform field to spatially localize the image signal from the different parts of a person's body was discovered by Paul.C. Lauterbur in 1973. And later on in 1974, Peter Mansfield developed the mathematics for fast scanning and image reconstruction. These two scientists were awarded the 2003 noble prize for Medicine or Physiology for their work.

1.3.4 The RF Coil

The magnetization vector is the sum total of the nuclear magnetic moments of each extra proton spin. The source of the signal is the fluctuation of the transverse magnetization in the person's body. The spins do not generate any signal as long as they are only subject to the main field $\vec{B}_0$ [9].

Therefore, to get a signal we need to disturb the magnetization or tip all the spins in the body part we chose to image. The spins or the magnetization is tipped (also called excited) by a radio frequency pulse that is generated by an RF coil from outside the persons' body.

Every time after being tipped, the magnetization vector gives a detectable signal as it relaxes back to its original equilibrium position from its transverse component. The RF coils are situated very close to the person's body to have the best proximity and then for better signal reception. Without disturbing the magnetization vector, no signal can be obtained and hence no imaging. RF fields are employed to tip or excite spins for both MRI and NMR spectroscopy. Fig.1.2 shows a schematic diagram of an MRI machine with the vital parts marked and their relative position indicated.

1.3.5 The Computer

MRI is inherently digital and it could not be performed without the digital computer. This is because the MRI signal does not interact directly with a medium that can be seen as an X-ray does. The MR signal does not present information in a form that can be directly viewed electronically, as it is done by an ultrasound.

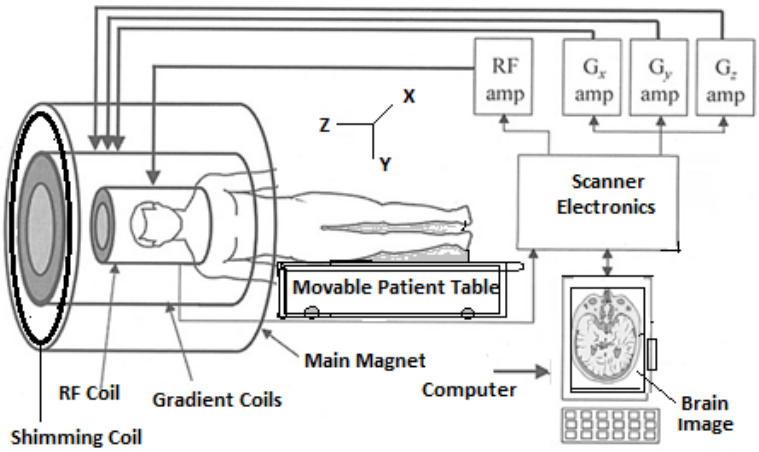

Figure 1.2: Schematic diagram of an MRI machine with main parts labeled

The repetitive continuous signal that we get from the fluctuation of the transverse magnetization vector is electronically collected and stored in a computer memory as a raw data and can not be seen directly.

Several mathematical and physical techniques are applied on the raw data to convert it into image and display on the screen. All this is done by employing proper application software and hence a specialized computer is a vital part of the MRI machine. The computer controls the gradient fields and the RF coils as well.

1.4 Precession and the Larmor Frequency

When the spins, each having magnetic moment $\vec{\mu}$, find themselves in the external static magnetic field $\vec{B}_0$, the magnetic moments of the spins and the main magnetic field interact and, as a result the spins experience a torque expressed as $\vec{\tau} = \vec{\mu} \times \vec{B}_0$, by the magnetic field $\vec{B}_0$. Because of the torque the spins rotate around the direction of the main static magnetic field. And this rotation is called precession. The spins precess around the direction of the main magnetic field with a certain angular frequency of precession $\vec{\omega}$ which can easily be derived from the geometry of the precession. This frequency of precession is called the Larmor frequency, after the theoretical physicist Sir Joseph Larmor. The Larmor angular frequency of precession (ω_0), measured in radian/sec, for the spins is given by

$$\vec{\omega}_0 = \gamma \vec{B}_0 \tag{1.2}$$

Here γ is called the gyro magnetic ratio of the proton and $\vec{B}_0$ is the static main magnetic field. The gyro magnetic ratio of a particle is defined as the ratio of the nuclear magnetic moment of the particle to its spin angular momentum given as

$$\gamma = \frac{\vec{\mu}}{\vec{J}} \tag{1.3}$$

$\vec{J}$ is the spin angular momentum of the precessing proton where it is given as $\vec{J} = \hbar I$ and the I is the intrinsic spin angular momentum quantum number which assumes the numerical value of $\frac{1}{2}$ for the proton.

The value of γ for the proton is $42.58 MHz/Tesla$ and it will have a Larmor frequency of 63.9MHz if the proton spin is found in a 1.5 Tesla external magnetic field [4]. We can express the Larmor frequency of precession in cycle per second (Hz) as

$$f_o = \frac{\gamma}{2\pi}\vec{B}_0 = \not{\gamma}\,\vec{B}_0, \tag{1.4}$$

where $\not{\gamma} = \dfrac{\gamma}{2\pi}$

The frequency of precession of the spins (the magnetization) depends on the strength of the static field.

1.5 Nuclear Magnetic Resonance Phenomenon

Nuclear magnetic resonance phenomenon is a phenomenon or a process by which the signal detected in MRI is generated. It is the phenomenon on which MRI is based [10]. To get a signal from the person inside the static field we have to disturb or tip the spins or the magnetization vector $\vec{M}_0$ from its equilibrium position using RF field of appropriate frequency. The magnetization vector can be disturbed however, if only the incoming RF field frequency exactly matches with the Larmor frequency of precession of the magnetization. When the two frequencies match, resonance occurs and this is called Nuclear Magnetic Resonance phenomenon between the frequency of the RF field (ω_{RF}) and the frequency of precession (ω_0) of the spins.

Only when $\omega_{RF} = \omega_0$, that is at resonance frequency, the RF energy is absorbed by the spins or by the magnetization vector and then the tipping takes place. If the frequency of the incoming RF field does not resonate with or is not tuned to the frequency of the precessing spins, no energy absorption and no tipping and no NMR.

When the RF field is applied the magnetization vector is tipped by an amount of angle θ depending on the strength of $\vec{B}_1$ and its lasting time. And θ is measured starting from the vertical axis (z axis) – along the lying person. This angle is called flip angle and is given by

$$\Delta\vec{\theta} = \gamma\vec{B}_1\tau, \tag{1.5}$$

where, γ is the gyro magnetic ratio of the proton, $\vec{B}_1$ is the RF field value, and τ is the time the RF field lasts.

1.6 The Relaxation Times

Consider a three dimensional space with x, y and z Cartesian coordinate system. The net or equilibrium magnetization vector $\vec{M}_0$, prior to disturbance, is oriented in the positive z direction in which the main magnetic field is directed as shown in Fig 1.3.

Next we turn on the RF field B_1, which is perpendicular to the $\vec{B}_0$ field and along the +x axis and for a very short period of time. We note that the resonance frequency should be such that $\vec{\omega}_{RF} = \vec{\omega}_0$. This time the magnetization vector will

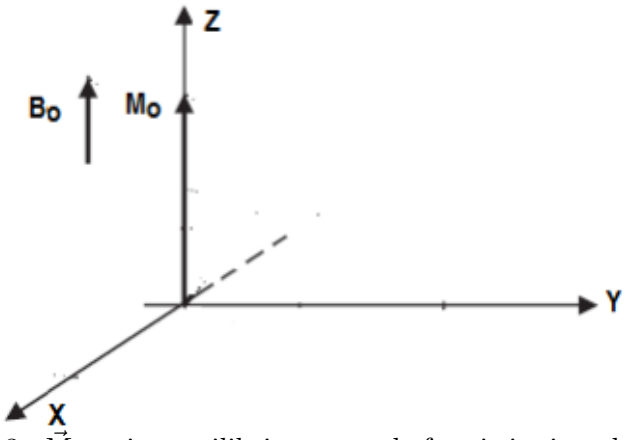

Figure 1.3: $\vec{M}_0$ at its equilibrium state before it is tipped by $\vec{B}_1$

be tipped towards the x-y plane by a certain flip angle θ as shown in Fig 1.4. in a rotating reference frame.

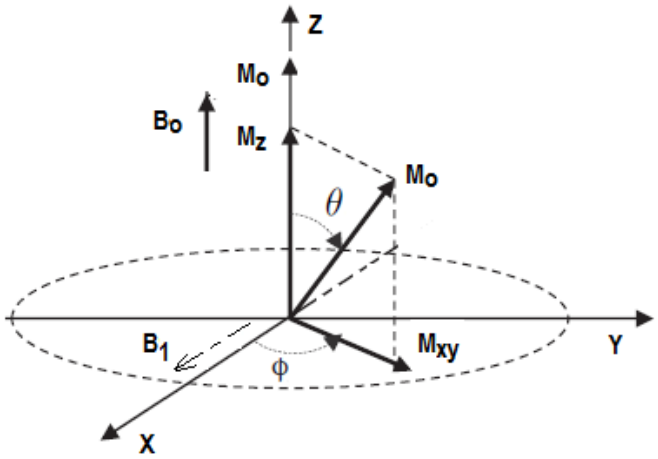

Figure 1.4: $\vec{M}_0$ flipped by $\vec{B}_1$ at resonance frequency $\vec{\omega}_{RF}$ by θ

The magnetization or the spins will be flipped away from the z axis as they precess down and around the $\vec{B}_0$ field. Fig 1.5 illustrates how a single proton spins on its own axis and also precesses around the main field $\vec{B}_0$. When the RF field is turned off, the magnetization vector returns back to its previous orientation by precessing upwards (along the z axis) after some time. When the magnetization is flipped it will be decomposed into two components. The components are the $\vec{M}_{xy}$ and the $\vec{M}_z$ as shown in Fig 1.4. Note that $\vec{M}_{xy}$ is the projection of $\vec{M}_0$ on to the xy plane. And the $\vec{M}_z$ is the projection of $\vec{M}_0$ on to the Z axis. By the law of vector addition we can write: $\vec{M}_0 = \vec{M}_{xy} + \vec{M}_z$.

And note that before tipping, $\vec{M}_0 = \vec{M}_z$ and $\vec{M}_{xy} = 0$. During tipping, $\vec{M}_z$ decreases and $\vec{M}_{xy}$ increases as $\vec{M}_0$ precesses around the B_0 down to the xy plane. Assuming a 90^0 flip angle, just after the RF is turned off, $\vec{M}_z$ starts to grow to $\vec{M}_0$ and $\vec{M}_{xy}$ starts to shrink to zero. To do so the magnetization vector precesses upwards. The $\vec{M}_z$ is called longitudinal magnetization and $\vec{M}_{xy}$ is called transverse magnetization. The RF field is put on and off many times and magnetization

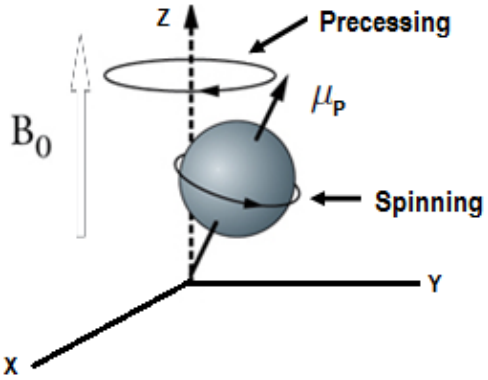

Figure 1.5: A proton spinning about its own axis and precessing around the main field at the same time

vector is tipped many times accordingly. In this way the motion of the magnetization precessing upward and downward is continuous and follows a complex helical trajectory as shown in Fig 1.6 in the laboratory frame.

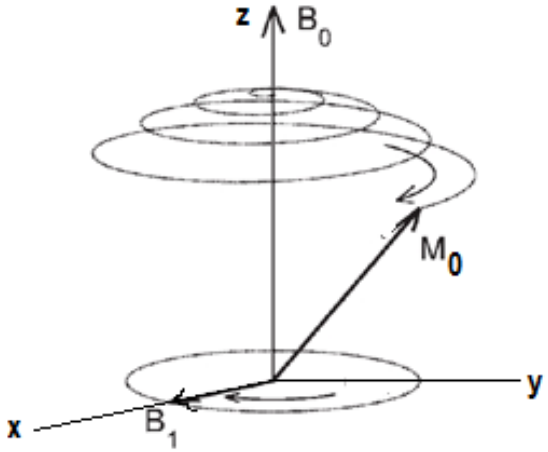

Figure 1.6: Trajectory of the magnetization vector under the $\vec{B}_0$ and RF ($\vec{B}_1$) fields: Helical in the lab frame of reference

This helical motion of the magnetization vector is what is happening in reality (that is as seen in a real laboratory frame of reference). In this case the magnetization motion is complex to discern. But, to make life simple we can choose and use a rotating frame of reference where we let the $\vec{B}_1$ field to rotate together with the magnetization. This means you (the observer) have to rotate with $\vec{B}_1$ at the resonance Larmor frequency $\vec{\omega}_{RF} = \vec{\omega}_0$, and watch what is happening.

The 90^0 angle of excitation, at this time, the complex motion of the magnetization is seen to be simple such that it only turns about a simple curve of 90^0 or a quarter of the circle as shown in Fig. 1.7, and repeats that every time the $\vec{B}_1$ field is on and off.

It is the transverse magnetization $\vec{M}_{xy}$ that is crucial to the generation of the MRI signal as it is measurable as it fluctuates under the successive and rapid tipping by the RF field. The longitudinal component$\vec{M}_z$ which is directed along the direction of the main field cannot be measured. This is because it is very small

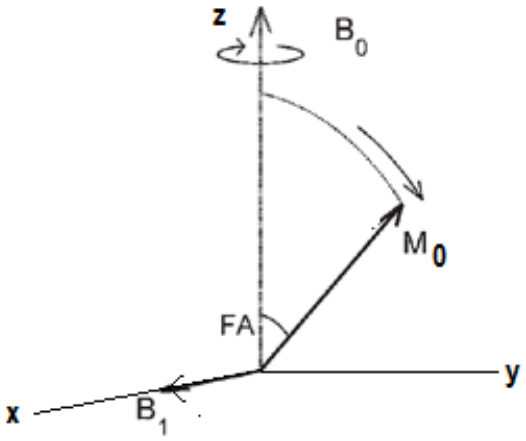

Figure 1.7: Trajectory of the magnetization vector under the $\vec{B}_0$ and RF ($\vec{B}_1$) fields.

as compared to the main field and hence difficult to isolate and measure.

Every time after the removal of the RF field, the time taken by the longitudinal magnetization $\vec{M}_z(t)$ to come back to its 63% of the equilibrium value of $\vec{M}_0$ is called relaxation time T_1 and it is shown in Fig 1.8. This time T_1 is also called spin - lattice relaxation time.

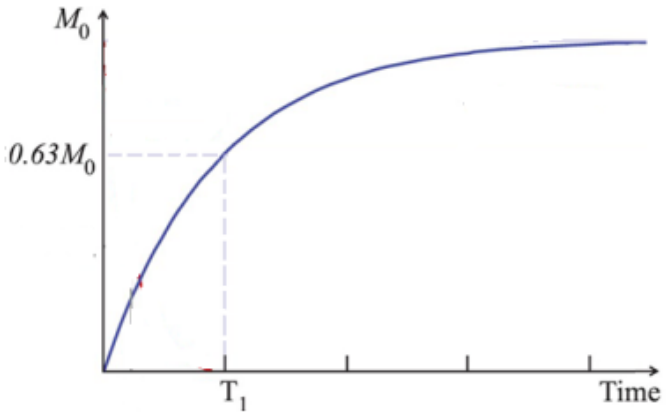

Figure 1.8: Relaxation time T_1 of the longitudinal magnetization vector $\vec{M}_z$ following RF tipping by 90^0. T_1 is recovery time for $\vec{M}_z$

And at the same time, the time taken for the transverse magnetization $\vec{M}_{xy}$ to shrink to 37% of its maximum value is called relaxation time T_2 and it is shown in Fig 1.9. This relaxation time T_2, is also called spin – spin relaxation time.

After a 90^o excitation, the longitudinal magnetization $\vec{M}_z(t)$ relaxes back to its equilibrium value as a function of time t given by the equation [11].

$$\vec{M}_z(t) = \vec{M}_0(0)(1 - e^{-\frac{t}{T_1}}), \tag{1.6}$$

Again following the 90^o excitation of the magnetization vector, the transverse magnetization component $\vec{M}_{xy}(t)$ relaxes to zero from its maximum value as a function of time given by the equation [11].

$$\vec{M}_{xy}(t) = \vec{M}_{xy}(0)e^{-\frac{t}{T_2}}, \tag{1.7}$$

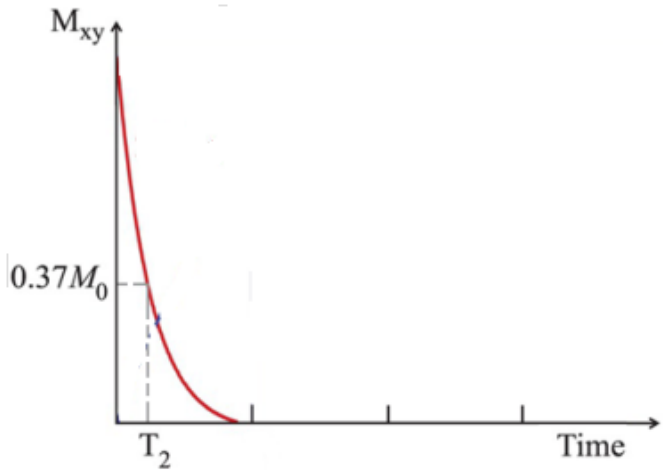

Figure 1.9: Relaxation time T_2 of the transverse magnetization vector $\vec{M}_{xy}$ following RF tipping by 90^0. It is decay time for $\vec{M}_{xy}$

T_1 - which is called the spin-lattice relaxation time, is due to interaction of the protons or spins with their surrounding or the neighboring lattice. In this time the spins give away energy, which they absorbed or acquired from the RF field during excitation, and while returning to their lowest energy state.

The T_2 - which is called spin-spin relaxation time, is due to the interaction between spins themselves in the x-y plane as they precess out of phase and cancel each other and reducing $\vec{M}_{xy}$ to zero.

In practice relaxations happen at the same time and they take place independent to each other. T_1 is longer than T_2 for any tissue. Every tissue has its own characteristics T_1 and T_2 values by which it is identified during imaging.

1.7 Bloch Equations

When the magnetization vector is tipped by an RF field it precesses down to the x-y plane. And when the RF field is off, it precesses upward and then comes back to its original value. This process continues and the magnetization vector executes a complex motion along a helical trajectory if seen in the lab frame or real situation.

The magnetization vector follows a simple curve if the observer rotates (in the rotating frame it looks stationary) along with the magnetization with the same Larmor frequency of precession as the magnetization vector does.

Bloch equations give us a mathematical description of the motion of the magnetization in both the lab and rotating frames of reference. Next the Bloch equations are explored from the point of view of a laboratory reference frame case by case.

1.7.1 Magnetization Interacting with only $\vec{B}_0$ field

In this case there is only one static field $\vec{B}_0$ acting on the spins or on the magnetization vector. The magnetization vector $\vec{M}_0$ experiences a magnetic force while being in the static field $\vec{B}_0$. This force creates a torque on it and makes it precess

around the $\vec{B}_0$ field. The magnetization $\vec{M}_0$ is the sum of the magnetic moments of the excess protons. Hence we can write the magnetization as

$$\vec{M} = \sum_i \vec{\mu}_i \tag{1.8}$$

Taking the time derivative of the magnetization gives

$$\frac{d\vec{M}}{dt} = \sum_i \left(\frac{d\mu_i}{dt} \right) \tag{1.9}$$

and using equation (1.3), that is $\vec{\mu} = \gamma \vec{J}$ we have

$$\frac{d\vec{M}}{dt} = \gamma \sum_i \frac{d\vec{J}}{dt}. \tag{1.10}$$

By Newton's 2nd law

$$\frac{d\vec{J}}{dt} = Torque = \vec{\mu}_i \times \vec{B}_0. \tag{1.11}$$

And after substitution (1.11) into (1.10) we get

$$\frac{d\vec{M}}{dt} = \gamma \sum_i \vec{\mu}_i \times \vec{B}_0 \tag{1.12}$$

And using equation (1.8), finally the Bloch equation for the magnetization vector which reacts with only $\vec{B}_0$ is given by

$$\boxed{\frac{d\vec{M}}{dt} = \gamma \vec{M} \times \vec{B}_0} \tag{1.13}$$

It is also possible to split and write the magnetization $\vec{M}$ and the static field $\vec{B}_0$ in terms of the rectangular coordinate components x, y and z. The static field is only along the z axis $\vec{B}_z$ and has no x and y components. So we can write component wise as: $\vec{M} = \vec{M}_x i + \vec{M}_y j + \vec{M}_z k$ and $\vec{B}_0 = \vec{B}_z k$. Then carrying out the curl product in equation (1.13), we get

$$\frac{d}{dt} \begin{vmatrix} \vec{M}_x \\ \vec{M}_y \\ \vec{M}_z \end{vmatrix} = \gamma \begin{vmatrix} i & j & k \\ \vec{M}_x & \vec{M}_y & \vec{M}_z \\ 0 & 0 & \vec{B}_z \end{vmatrix} = \gamma(\vec{M}_y \vec{B}_z) i - \gamma(\vec{M}_x \vec{B}_z) j \tag{1.14}$$

Splitting equation (1.14) into the three components we get

$$\frac{d\vec{M}_x(t)}{dt} = \gamma \vec{M}_y(t) \vec{B}_z \tag{1.15}$$

$$\frac{d\vec{M}_y(t)}{dt} = -\gamma \vec{M}_x(t) \vec{B}_z \tag{1.16}$$

$$\frac{d\vec{M}_z(t)}{dt} = 0 \tag{1.17}$$

If we let $\omega = \gamma \vec{B}_z$, then the solution for the components, $\vec{M}_x$, $\vec{M}_y$ and $\vec{M}_z$ as a function of time becomes

$$\vec{M}_x(t) = \vec{M}_x(0)\cos(\omega t) + \vec{M}_y(0)\sin(\omega t) \tag{1.18}$$

$$\vec{M}_y(t) = \vec{M}_y(0)\cos(\omega t) - \vec{M}_x(0)\sin(\omega t) \tag{1.19}$$

And:

$$\vec{M}_z(t) = \vec{M}_z(0) \tag{1.20}$$

Equations (1.18) to (1.20) describe the time evolution of the magnetization vector components as a function of time around the main field. The components can be added together to yield the one Bloch equation for the magnetization as it is reacting only with the static magnetic field. And that is given as

$$\boxed{\frac{d\vec{M}(t)}{dt} = \gamma \vec{M}_y(t)\vec{B}_z i - \gamma \vec{M}_x(t)\vec{B}_z j} \tag{1.21}$$

Next we shall see the Bloch Equation for the motion of the magnetization vector when the relaxation times T_1 and T_2 are added and considered.

1.7.2 Magnetization Interacting with $\vec{B}_0$, T_1 and T_2

As discussed previously, the relaxation times, T_1 and T_2 take place at the same time but independently. The T_2 is very short than T_1. In addition, T_1 and T_2 differ from tissue to tissue and they affect the way the magnetization vector moves around the main field.

Now we take the two spin-lattice and spin-spin relaxation processes and their corresponding relaxation times T_1 and T_2 into consideration and include them in to Bloch equation. The relaxation process is a process in which the non – equilibrium magnetization $\vec{M}_z$ (where $M_x \neq 0$, $M_y \neq 0$ and $M_z \neq M_0$) attains the equilibrium magnetization (where $M_x = 0$, $M_y = 0$ and $M_z = M_0$) after sufficiently long time.

The spin-lattice relaxation process involved energy exchange between the spins and the surrounding while the spin-spin relaxation process does not involve exchange of energy with the surrounding. And hence the two processes are characterized by different time constants. For this physicist Flex Bloch assumed and proposed that the two processes to be first order processes stating mathematically as [12].

(i) For the transverse relaxation process

$$\frac{d\vec{M}_x(t)}{dt} \propto -\frac{\vec{M}_x}{T_2} \tag{1.22}$$

and

$$\frac{d\vec{M}_y(t)}{dt} \propto -\frac{\vec{M}_y}{T_2} \tag{1.23}$$

(ii) For the longitudinal relaxation process

$$\frac{d\vec{M}_z(t)}{dt} \propto -\frac{(\vec{M}_z - \vec{M}_0)}{T_1} \tag{1.24}$$

And next by combining equations (1.15) to (1.17) with the corresponding equations (1.22) to (1.24), we get
(a) for transverse relaxation

$$\frac{d\vec{M}_x(t)}{dt} = \gamma \vec{M}_y(t)\vec{B}_z - \frac{\vec{M}_x}{T_2} \tag{1.25}$$

and

$$\frac{d\vec{M}_y(t)}{dt} = -\gamma \vec{M}_x(t)\vec{B}_z - \frac{\vec{M}_y}{T_2} \tag{1.26}$$

(b) For the longitudinal relaxation

$$\frac{d\vec{M}_z(t)}{dt} = -\frac{(\vec{M}_z - \vec{M}_0)}{T_1} \tag{1.27}$$

Equations number (1.25) to (1.27) describe the motion or the time evolution of the magnetization vector with the relaxation time constants T_1 and T_2 included. And combining the three components the Bloch equation for the magnetization vector with the relaxation times and the static magnetic field is given as [11].

$$\frac{d\vec{M}}{dt} = \vec{M} \times \gamma\vec{B} - \frac{\vec{M}_x i + \vec{M}_y j}{T_2} - \frac{(\vec{M}_z - \vec{M}_0)k}{T_1} \tag{1.28}$$

In equation (1.28) the first term on the right side of the equal sign represents the precession process. The second and the third terms represent the transverse decay and longitudinal recovery processes respectively.

1.7.3 Magnetization Interacting With $\vec{B}_0$, $\vec{B}_1$, T_1 and T_2

Now we shall consider the effect of an additional magnetic field on the motion equation of the magnetization vector. This field is the tipping RF field $\vec{B}_1$ with a frequency of oscillation ω_1 which is applied in the transverse x-y plane perpendicular to $\vec{B}_0$. With the addition of the RF field $\vec{B}_1$, the equations that govern the motion of the magnetization vector changes. Firstly, the $\vec{B}_1$ RF field can be assumed to change along the x-y plane as a function of time governed by the relation

$$\vec{B}_1(t) = \vec{B}_1 \cos(\omega t)i + \vec{B}_1 \sin(\omega t)j, \tag{1.29}$$

with the addition of the RF filed $\vec{B}_1$ the total magnetic field acting on the magnetization vector becomes , $\vec{B}_{eff} = \vec{B}_1(t) + \vec{B}_0 k$ and is given as

$$\vec{B}_{eff}(t) = \vec{B}_1 \cos(\omega t)i + \vec{B}_1 \sin(\omega t)j + \vec{B}_0 k \tag{1.30}$$

This above expression for the total magnetic field $\vec{B}_{eff}(t)$ acting on the magnetization can be substituted in equation (1.25) and (1.26) in place of $\vec{B}_z$ and then

the equation can be solved to give the expression for the time dependence of the motion of the magnetization vector in the additional presence of the oscillating RF field $\vec{B}_1$. Accordingly, the general Bloch equation along the components x, y and z, in the real situation (lab frame) is given by
(i) For the transverse motion along x

$$\frac{d\vec{M}_x(t)}{dt} = \gamma \vec{M}_y(t)\vec{B}_0 + \gamma \vec{M}_z \vec{B}_1 \sin(\omega t) - \frac{\vec{M}_x}{T_2} \tag{1.31}$$

(ii) For the transverse motion along y

$$\frac{d\vec{M}_y(t)}{dt} = \gamma \vec{M}_z(t)\vec{B}_1 \cos(\omega t) - \gamma \vec{M}_x \vec{B}_0 - \frac{\vec{M}_y}{T_2} \tag{1.32}$$

(iii) For the longitudinal relaxation process along z

$$\frac{d\vec{M}_z(t)}{dt} = -\gamma \vec{M}_x(t)\vec{B}_1 \sin(\omega t) + \gamma \vec{M}_y \vec{B}_1 \cos(\omega t) - \frac{(\vec{M}_z - \vec{M}_0)}{T_1} \tag{1.33}$$

Equations (1.31) to (1.33) describe the way the components of the magnetization along the x, y and z axes in the laboratory frame of reference. The equations represent the complex dynamics of the magnetization which is shown in Fig. 1.6.

1.8 MRI Signal and the Transverse Magnetization

The moment the magnetization vector is flipped into the x-y plane, we get a changing transverse magnetization. This changing magnetization vector is equal to changing magnetic field. To pick the signal we place a coil of wire or an antenna perpendicular to the transverse magnetization as shown in Fig 1.10(a). This creates a magnetic flux change through the coil and consequently, by Faraday's law of EM induction, a variable or sinusoidal electric voltage and current will be induced in the coil.

This sinusoidal electric voltage or current is the MRI signal (in its analog form) that carries the image information of the tissue. A simplified diagram of the mechanism of the signal reception from the time varying transverse magnetization is been in Fig 1.10.

The moment the RF field is on, the $\vec{M}_{xy}$ is maximum. When the RF is just off, the $\vec{M}_{xy}$ starts to decline or decay quickly with time. That decaying signal is shown in Fig. 1.10(b). We have to collect it quickly before it becomes zero and this signal which we get after a single RF pulse is called free induction decay (FID). The $\vec{M}_{xy}$ rotates with in the x-y plane at Larmor frequency when it generates the FID. The greater is the $\vec{M}_{xy}$ the greater is the intensity or amplitude of the signal or the FID.

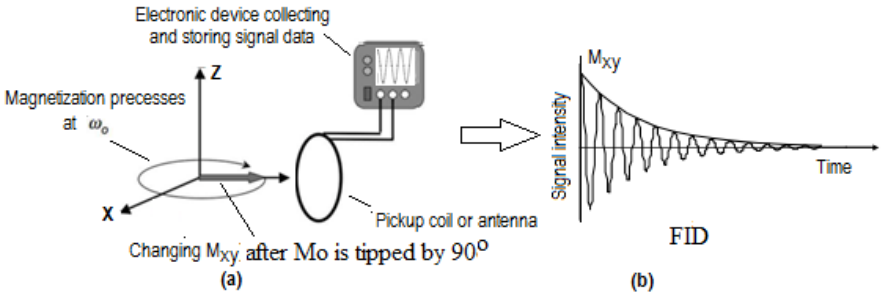

Figure 1.10: Schematics diagram of signal detection and collection mechanism

1.9 Signal Processing and Imaging Procedure

1.9.1 The K Space

The MRI signal is sinusoidal infinite and continuous. In reality since the computer does not work with continuous values we have to change this signal into discrete and finite values. To do so we take samples of the continuous signal and store it as an array of numbers. This sample array of numbers is called k-space and it is finite and discrete raw data stored in a computer memory.

This data or k space represents the spatial frequency information of each unit volume of spins (voxel) and hence information of the image. It is arranged in a form of rectangular matrix of numbers.

Then next we have to apply a mathematical technique called inverse Fourier transform (IFT) on the raw data of k space in order to obtain the image we need. To change the image data back to the k space we apply the Fourier transform (FT). Examples of the k space and the corresponding image space are shown in Figure 1.11. The images belong to a person's brain and a zebra's face respectively.

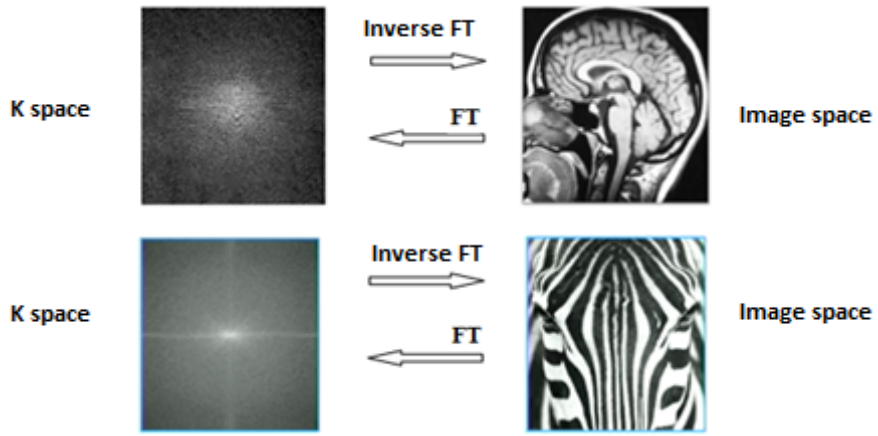

Figure 1.11: Transformation between k space and image space

1.9.2 Fourier Transform and MRI Signal

The Fourier transform is a mathematical technique used to express any waveform or signal as an infinite sum of sines and cosines by changing the waveform or

signal from its time domain to its frequency domain. To convert the frequency domain expression of the signal to the time domain expression, the inverse Fourier transform is used. This mathematical technique is well known and developed many years ago before MRI was discovered. The Fourier transform has got several established properties that can be used in MRI.

Fortunately, the MRI signal $s(k)$ which is sampled and stored in the k-space (representing raw data) and the spin density $\rho(x)$ in the position space (representing the image) of the small volume of tissue (voxel) are found to be related inversely in Fourier transform. The raw signal (in k space) is equal to the Fourier transform of the spin density $s(k)$. And the spin density is equal to the inverse Fourier transform of the k space data. In two dimensions the mathematical relationship between $s(k_x, k_y)$ and $\rho(x, y)$ is given by the following formula [13].

$$s(k_x, k_y) = \int_{-\infty}^{\infty}\int_{-\infty}^{\infty} dxdy\, \rho(x, y)e^{-j2\pi(k_x x+k_y y)} \tag{1.34}$$

And

$$\rho(x, y) = \int_{-\infty}^{\infty}\int_{-\infty}^{\infty} dk_x dk_y\, s(k_x, k_y)e^{j2\pi(k_x x+k_y y)} \tag{1.35}$$

This means we can get the spin density in the position space or get the image of the object by carrying out the inverse Fourier transform operation on the signal in k-space. Therefor the mathematical techniques of Fourier transform is so vital to MRI. In addition the different properties of Fourier transform such as shifting, scaling, and convolution have direct application in the processing of MRI signal to form the images.

1.9.3 Signal-To-Noise Ratio (SNR)

In MRI the signal we measure is always equal to the sum of the pure signal that is related exactly to the image (that is from the spins in the tissue) and a kind of signal that is not related to the image (that is coming from different source or the surrounding environment). This second type of signal is not needed and hence it is called noise. The quality of the image we get hence depends on the relative presence of the pure signal and the noise we measure inevitably. This is because mostly signal and noise come intermingled.

The quantity SNR or the signal – to – noise ratio determines the level of clarity and quality of the image. To get a better image the signal should be pronounced much more than the noise. The SNR mathematically is defined as

$$SNR = \frac{Signal\,Amplitude}{Standard\,Deviation\,of\,the\,Noise} = \frac{Signal}{\sigma} \tag{1.36}$$

The noise comes from different sources. And the factors that influence the SNR in MRI could be the strength of B_0, the way the RF coil is designed, the spin or proton density of the tissue, the size of the pixel and that is the product $(\delta x)(\delta y)$ and others.

1.9.4 Contrast-To-Noise Ratio (CNR)

Contrast to noise ratio is the difference in respective SNR of two different tissues to be imaged. Mathematically

$$CNR = SNR_A - SNR_B \tag{1.37}$$

SNR_A and SNR_B are signal- to- noise ratios of two tissues A and B respectively. The greater is the difference in their SNR, the greater is the contrast to noise ratio and the better is the distinction between the two tissue types. As we learn from the above equation for CNR, it is the difference between the SNR of the tissues that contributes to the CNR. This means to enhance the CNR and get a better perception of the differences we need to suppress the SNR of either one of the tissues A or B using different techniques.

1.10 Recent Developments in MRI Technology

Ever since MRI machine was used for imaging, researchers in the field had been and are investigating for ways of improving the different shortcomings of the technology. Some shortcomings of the technology were: the high sound heard during scanning, the lengthy time of scanning, difficulty to get an image of the lung, the closed bore of the MRI machine triggering claustrophobic fear in the patient and potential patient body reactions to the frequently varying gradient fields such as peripheral nerve stimulation.

As the research continues a new development of relevant software technology has recently enabled the fast contrast scanning and resulting in simplification of the cardiac imaging work flow and reducing the scanning time. In addition the scanning of the lung has now been possible which was difficult before because of the low content of hydrogen atoms in the air filled lung [6].

The possibility of using a very high magnetic field such as more than 7 tesla was previously used for only research purposes. This was because the effect of very high field on patients was not well studied. But now recently research has got it possible to use 7 Tesla magnetic field strength for clinical use. In addition open bore MRI machines are being constructed as an alternative and this could alleviate the fear by some patients, of being confined in the cylindrical scanner.

The GE (General Electric) SilentScan MRI noise reduction technology has been in use with a 3 Tesla field system, that greatly reduce noise during MRI scans. The GE has also introduced the so called AIR coil technology which is substituting the common RF coils placed near the patient body. The AIR[2] coil technology, unlike the conventional RF coils, provides comfort for patients, improves signal reception and enable better coil positioning among others.

1.11 Optical Coherence Tomography (OCT)

Optical coherence tomography (OCT) is an imaging technique that allows rapid and non-invasive acquisition of high-resolution images of the retina [14]. This

[2]Watch video: https://www.youtube.com/watch?v=8-OqKSEqDqI

technique can be used as an alternative to MRI for several parts of the body such as the eye as well as for tissue imaging.

It is used to identify tissue problems such as multiple sclerosis (MS) with high image spatial resolution and can play a complementary role to MRI by offering additional useful information. In terms of the time taken for image acquisition and as well as cost, OCT is better than MRI. OCT has similarity to the way an ultrasound imaging functions but uses LASER. OCT is used widely in ophthalmology [3].

1.12 Safety First

1.12.1 Introduction

Magnetic resonance imaging examination by itself is harmless and poses no risk as discussed before. However, proper and careful usage of the magnetic system and its environment is essential. As a result before and during the time of clinical MRI examinations, there are several safety procedures to consider in order to ensure complete patient safety. The care that should be taken not only applies to the patient but also to the medical staff and the radiologist that work in the scanning room. If proper care is not established potentially very serious accidents raging from physical hurt to the level of death can occur.

1.12.2 Magnetic Materials

It is known that the MRI machine uses very strong magnetic field for its operation. The magnetic field can exert a tremendous force in attracting any nearby magnetic material and pull it into the bore very quickly. If magnetic materials are attracted to the bore of the magnet the moving materials can cause a serious harm on the patient or the person in the room.

Several MRI scanning room accidents have been registered since the start of using the machine for imaging. Once up on a time, it was recorded that a police office's pistol was snatched away out of the pistol's case on the officer's belt and the bullet was fired on the wall as the pistol collided with the magnet. [15]. A record shows that an Indian man died as a result of an accident that occurred as he was taking an oxygen metal tanker into the MRI scanner room.

Therefore there are several safety procedures to be followed to ensure safe scanning. Accordingly, anyone (patient or the medical staff) who is about to enter the magnetic field should be well screened or checked for the following things

- Metallic objects

  Check for any metallic object that is implanted in the body as a medication for some health problem such as: Pace makers, intra-ocular foreign bodies, cochlear and spinal implants

  This is because the medical devices that are implanted contain metallic things such as tiny wires and so can be snatched out of the patient body and

[3] ophthalmology is the scientific study of the eye and the associated diseases

pose further danger. So persons with metallic objects in their body cannot be examined with the machine.

- Possibility of early pregnancy

  In the time of early three months of a woman's pregnancy (trimester), unless it is a must for the sake of the women's health, MRI examination is not advisable as it can disturb the normal fetus development.

- Removal of any jewelry, credit card, money, watches, any ferromagnetic object that contains iron or steel from the external body parts of the person or from their purse or pocket.

It is important to prepare a check list or screening form so that everybody that is patients and relatives or other people may be checked before the examination takes place and to guarantee patient care. If the proper care is not taken, injury or even fatal accidents may occur. It is also good to accompany the patient for some time for a rare possible reaction of the patient after examination until he/she is well back to their previous situation.

An overall patient care not only includes magnetic safety but also includes consideration of the past and present patient medical condition. Besides, the creation of relaxing examination room or scanning environment and a smoothly running facility is essential.

1.12.3 RF and Gradient fields

There is also a safety issue associated with the usage of the RF and Gradient fields during scanning. There are regulatory limits to the amount of safe body absorption rate of RF field power called specific absorption rate (SAR) [16]. If RF field is not used up to the regulatory limit, high absorption of RF by the patient may cause the production of heat on the person's body which potentially can trigger unpleasant heating sensation.

The possibility of unnecessary peripheral nerve or tissue stimulation which may result in muscle twitching and pain is also the other safety concern that may occur due to very quick switching of the gradient fields [17]. There is, however rare danger due to these fields because of an inbuilt safeguard. Nevertheless, the MRI machine parts should always be checked for proper functioning and any malfunctioning component should be immediately repaired.

1.13 Organization of the Thesis

This thesis is organized into four chapters. The first chapter provides a general overview of what an MRI machine is, as one of the many medical diagnostic tools, and explains the basic physical principles for its functioning. The second chapter, as a review of related literature, is all about determination of electric field inside a solid sphere which is taken as a model for the human head. The electric field determination is essential in the process of the treatment process called transcranial magnetic stimulation (TMS). The third chapter , which contains the core problem of the thesis, focuses on the determination of the distribution of the magnetic field,

electric field and eddy current density inside a solid cylindrical volume conductor which is caused during MRI scanning of a patient by the time varying Z gradient field. Chapter four gives a summary of the main points of this thesis as well as discusses on directions for future related work.

1.13.1 Motivation

Magnetic resonance imaging machine, in addition to possessing a strong and static magnetic field, it also utilizes gradient fields which vary very quickly as a function of time. This means the patient is exposed to the strong and static magnetic field and to the time dependent gradient magnetic fields. By Faraday's law a time varying magnetic field induces electric eddy current inside a conducting media such as human body. This current may interact with the body tissue and induce some effect on it. The motivation of the study comes from the need to study the behavior and interaction of the eddy current with the tissue. The understanding of the behavior of the induced eddy current distribution inside a patient's body may prove beneficial to securing the safety of the patient in controlling and protecting possible stimulation of the peripheral nerve and provides useful information to the effort made to design better gradient coil.

1.13.2 Objective of the Thesis

The objective of the thesis is to explore the behavior of the induced electric field and eddy current density which is caused by the fast switching frequency of MRI Z gradient field inside a solid cylindrical volume conductor (human body model) and to investigate the effect and relationship of the eddy current density with peripheral nerve stimulation.

CHAPTER 2
REVIEW OF RELATED LITRATURE

2.1 Magnetic Stimulation of the Brain (CNS)

The brain can be stimulated using an induced time varying magnetic field pulse without causing pain [18]. The varying magnetic field can pass through the scalp and skull of the head and hence there is no need to make surgery. The method is therefore called non-invasive.

By Faraday' law of electromagnetic induction, the time varying magnetic field induces an electric field inside the brain. The induced electric field in turn induces current in the brain. And the current finally causes stimulation of the brain tissue or the brain cell (Neuron). The time varying magnetic field can be generated by passing a changing electric current pulse through a coil of wire situated near the head. See figure 2.1. below.

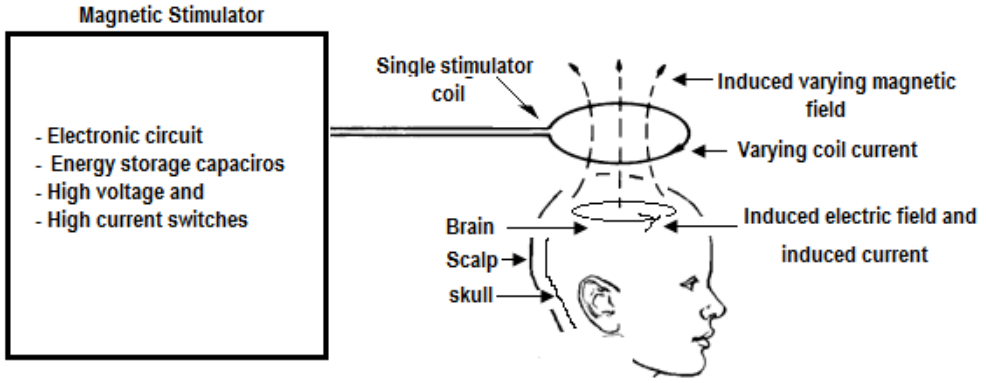

Figure 2.1: Basic diagram of magnetic nerve stimulator

Stimulation, in here, refers to the process or action of activating any abnormally behaving brain tissue or brain cell so that it can be made to start its normal and natural work by a magnetic field. Magnetic stimulation has been used for the purpose of research since long time ago. Besides, it is used clinically for the purpose of diagnostics and treatment of several brain disorders such as depression and epilepsy [19]. In the brain cortical cells are stimulated by strong magnetic field pulses that can induce a flow of current in the tissue which leads to membrane depolarization and there by neural excitation [20].

2.2 The Theory of Volume Conductors

Biological materials consisting of biological tissue conduct electricity. But they have several distinguishing features from the physical electrical conductors we commonly know such as wires and electrolytes. To study bioelectric and bio-magnetic processes and phenomena, the conducting media we deal with are the

biological materials called *volume conductors*. Such conductors are the heart, the brain, the human body and other body parts of a biological entity. In a volume conductor we do not have an inductor like the physical circuit element. But there are resistances, electric potential sources (like batteries) and capacitances but which are not discrete as in the physical circuit elements [21].

In a volume conductor the batteries (bio-electric sources), the resistances and the capacitances are distributed continuously in all directions in the volume conductor medium. Any biological body or body part has its own natural current sources. This means it creates its own electric currents and hence it produces magnetic field. All communication activities in the body are carried out by using electrical and chemical signals in the body.

2.3 The Challenge with Magnetic Stimulation

The fundamental problem of transcranial magnetic stimulation (TMS) is determining the site and size of the stimulated cortical area [22]. This is because magnetic stimulator coils fall short of focusing exactly at a required area of interest. The stimulation includes more area than the required spot. This is not needed and hence the situation has to be improved. One step towards achieving precise focusing to stimulate only the required region of interest is to determine and understand the induced electric field and the current density distributions at any point in the brain as easily and quickly as possible.

2.4 Calculation of the Induced Electric Field inside the Brain

2.4.1 Modelling the Head

In reality the head is not a perfect sphere. It is neither homogeneous nor isotropic. But to make the mathematics simpler it is necessary to make approximations. Several researchers have adopted different models for the head in order to compute the induced electric field in it. For example Rush and Driscoll introduced the three sphere model of the head. That is a sphere having three concentric layers to represent the scalp, skull and the brain [23]. Regarding the induced electric field, several researchers have adopted several approaches in order to compute the field. For example, some have ignored the conductor boundary [24]. Others have treated the conductor boundary as an infinite hall space [25]. Still others have adopted a quasispherical volume applying the FE technique [26]. And also the three-sphere model was used employing the FD approximation technique [27]. Both the FE (finite element) and FD (finite difference) are approximation methods involving numerical techniques to solve differential equations.

In all the above cases the result of the induced electric field comes from specific coil shape and orientation to the head. Where as in practice the desired coil shape and placement during brain magnetic stimulation, may not conform to any of the above specific coil shapes and placements. Because the coil shape and placement has been deemed specific. However, researchers such as AMASSIAN et al., 1989;

COHEN, L. G. et al., 199l; MEYER et al., 1991 ; and UENO et al., 1990 [28–31], have investigated experimentally to determine the effect of coil orientation on brain stimulation. Here a single sphere, isotropic and homogeneous head model has been assumed.

This paper presents a mathematical method which enables us to calculate directly the electric field inside a homogeneous spherical volume conductor not for a specific coil shape and orientation, but for any practical excitation arbitrary coil shape and orientation. The method is simple and takes little time for computing the electric field with a PC. If the electric field distribution is known everywhere in the brain, then by applying the reciprocity theorem, MEG problems can also be dealt with. This is because TMS and MEG are inverse processes.

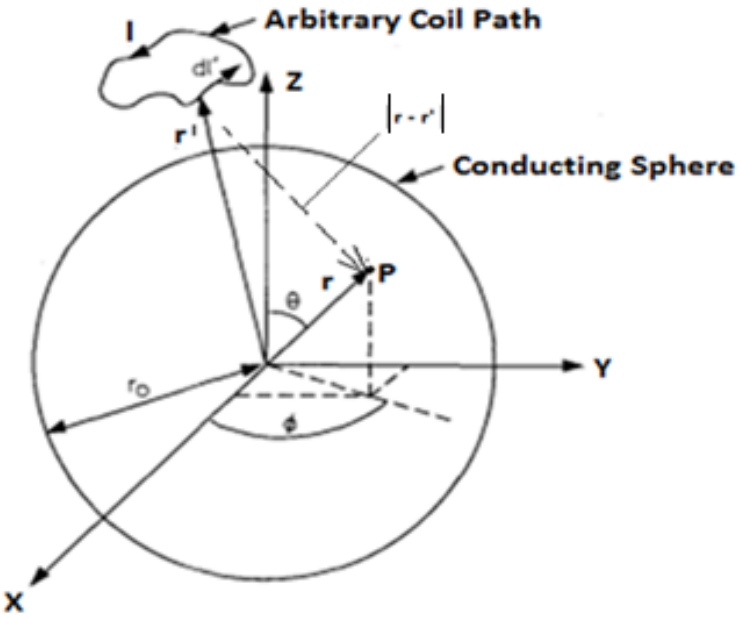

Figure 2.2: Spherical model of the head

2.4.2 Parametric Assumptions

The chosen spherical model of volume conductor has been assumed to be homogeneous and isotropic and to have permeability of free space μ_0, electrical permittivity ϵ_s and conductivity σ. Outside the spherical volume the conductivity is assumed to be zero and the electrical permittivity will be equal to that of free space. (That is $\epsilon = \epsilon_0$). In addition, the current in the arbitrary coil is assumed to flow in a negligible filament of wire found at the center of the wire. Since the frequency of excitation $f = \dfrac{\omega}{2\pi}$ is taken to be very low, the propagation effect and the skin depth in the spherical volume conductor have been ignored. This assumption implies that the coil size should not be much greater than the head of radius r_0.

2.4.3 Derivation of the Induced Electric Field Equations

The current through the arbitrary coil produces magnetic vector potential $\vec{A}$ around and in the sphere model of the brain. This vector potential $\vec{A}$ gives rise to a magnetic field $\vec{B}$ in the brain. Since the current pulse that passes through the coil is changing in time, the magnetic field is also changing in time. By Faraday's law a changing magnetic field produces an electric field in the brain. From Gauss' law we have the fact that $\nabla \cdot \vec{B} = 0$. And this means there is no magnetic mono pole. Mathematically this implies that the magnetic field vector can be obtained from the coil current vector potential A as follows

$$\vec{B} = \nabla \times \vec{A} \tag{2.1}$$

But the vector potential A is given by the closed loop integral formula

$$\vec{A} = \frac{\mu_0}{4\pi} \oint_{coil} \frac{Idl'}{|r - r'|}, \tag{2.2}$$

where

I = current in the arbitrary coil,
dl' = differential length of the coil to be integrated,
r = distance from the center of the coordinate to the field point P.
r' = distance from the center of the coordinate to the differential vector length to be integrated or source point
$|r - r'|$ = distance from the differential vector current length to the field point P.

According to Faraday's law of EM induction we have

$$\vec{\nabla} \times \vec{E} = -\frac{\partial \vec{B}(t)}{\partial t} \tag{2.3}$$

But since the magnetic field B is time harmonic, we can use its frequency domain expression $\vec{B}(t) = \vec{B}e^{j\omega t}$ and then after substitution we get the expression

$$\frac{\partial \vec{B}(t)}{\partial t} = \frac{\partial}{\partial t}\left(\vec{B}e^{j\omega t}\right) = j\omega\vec{B} \tag{2.4}$$

Substituting the above result in Faraday's law yields

$$\vec{\nabla} \times \vec{E} = -\frac{\partial B(t)}{\partial t} = -j\omega\vec{B} \tag{2.5}$$

Since $\vec{B} = \vec{\nabla} \times \vec{A}$

$$\vec{\nabla} \times \vec{E} = -j\omega(\vec{\nabla} \times \vec{A}) \tag{2.6}$$

$$\vec{\nabla} \times \vec{E} + j\omega(\vec{\nabla} \times \vec{A}) = 0 \tag{2.7}$$

$$\vec{\nabla} \times (\vec{E} + j\omega\vec{A}) = 0 \tag{2.8}$$

If the curl of the quantity in the bracket (2.8) is zero, it means the quantity in the bracket can be expressed as being equal to the negative gradient of a scalar

potential V, that is

$$(\vec{E} + j\omega\vec{A}) = -\vec{\nabla}V \tag{2.9}$$

$$\vec{E} = -j\omega\vec{A} - \vec{\nabla}V \tag{2.10}$$

Since, $j\omega\vec{A} = \dfrac{\partial\vec{A}}{\partial t}$, equation (2.10) can be written as

$$\vec{E} = -\frac{\partial\vec{A}}{\partial t} - \vec{\nabla}V \tag{2.11}$$

Equation (2.11) shows that the induced electric field inside the spherical volume conductor (the brain), comes from two sources [32]. The first source is the magnetic vector potential $\vec{A}$ generated by the coil current and the second source is the electric scalar potential V generated by the static charge which is accumulated on the surface of the spherical conductor [28]. This means, also for this isotropic and homogeneous volume conductor model, the coil geometry affects the quantity $\dfrac{\partial\vec{A}}{\partial t}$, and the geometry of the boundary affects the gradient of the scalar potential $(\vec{\nabla}V)$ [33]. Hence to calculate the electric field at any place inside the head, it is necessary to calculate the vector potential and the scalar potential at the specific point of interest. The magnitude of the electric field due to the coil current depends on the rate of change of the current in the coil and its distribution is dependent on the shape or coil geometry.

The scalar potential V in equation (2.11) satisfies Laplace's equation (i.e $\nabla^2 V = 0$) inside the spherical volume conductor [34]. This is because there is no volume charge density inside the spherical volume conductor. And since the choice of coordinate in here is spherical, Laplace equation in spherical coordinates is given as

$$\nabla^2 V = \frac{1}{r^2}\frac{\partial}{\partial r}\left(r^2\frac{\partial V}{\partial r}\right) + \frac{1}{r^2\sin\theta}\frac{\partial}{\partial\theta}\left(\sin\theta\frac{\partial V}{\partial\theta}\right) + \frac{1}{r^2\sin^2\theta}\left(\frac{\partial^2 V}{\partial\phi^2}\right) = 0 \tag{2.12}$$

Next we need to solve for the scalar potential V from equation (2.12). To do so, first we employ the separation of variables to extract three equations from equation (2.12) that are dependent on r, θ, and ϕ. The three equations we get will be: R(r), $\Theta(\theta)$ and $\Phi(\psi)$.

The equation dependent on r is

$$r^2\frac{d^2R}{dr^2} + 2r\frac{dR}{dr} - l(l+1)R = 0 \tag{2.13}$$

The equation dependent on θ is

$$\frac{d^2\Theta}{d\theta^2} + \frac{\cos\theta}{\sin\theta}\frac{d\Theta}{d\theta} - \frac{m^2}{\sin\theta} + l(l+1)\Theta = 0 \tag{2.14}$$

The equation dependent on ϕ is

$$g(\phi) = \frac{1}{\Phi}\frac{d^2\Phi}{d\phi^2} = -m^2 \tag{2.15}$$

The next step is that, to get the complete solution for the scalar vector potential

V(r,θ,ϕ), we need to solve the ordinary differential equations (2.13), (2.14) and (2.15). Solving for R(r) from the radial dependent equation (2.13) we get the solution

$$R(r) = Ar^{l} + Br^{-}l + 1 \tag{2.16}$$

A and B are complex constants. Solving for Θ from the θ dependent equation (2.14) we get the solution

$$\Theta(\theta) = P_l^m \cos\theta \tag{2.17}$$

However, the solution for equation (2.14) is available if only the value of 'l' is equal to some integer. And these solutions for this equation (2.14) are Legendre's polynomials as shown in equation (2.17) above. Next, solving for Φ from the azimuthal angle dependent equation (2.15) we get the solution

$$\Phi(\phi) = e^{\pm jm\phi} = C\sin(m\phi) + D\cos(m\phi), \tag{2.18}$$

where m= 1,2,3,...
Here the solution function Φ describes the potential of the static charge distribution that resides on the sphere surface. And its azimuthal dependence is periodic over a period of 2π. Then the general solution of the main Laplace's equation (2.12) is the product of the solutions (2.16), (2.17) and (2.18). That is V(r,θ,ϕ)=R(r)$\Theta(\theta)\Phi(\phi)$. And accordingly, the general solution for the Laplace's equation in spherical coordinates can be expressed by the relation [35].

$$V(r,\theta,\phi) = \sum_{l=0}^{l=\infty} \sum_{m=-l}^{m=l} \big(F_{lm} r^{l} + G_{lm} r^{-(l+1)}\big) Y_{lm}(\theta,\phi), \tag{2.19}$$

where the $F_{lm} = A$ and $G_{lm} = B$ are complex constants, with, m=1,2,3,.. and Equation (2.19) gives the scalar potential at any point as a function of r, θ and ϕ. To get the potential values inside and outside the spherical volume and then to get a unique solution, boundary conditions have to be imposed on the general solution (2.19). Accordingly, the one condition is that, as r decreases to zero (at the coordinate origin), the potential inside should be finite and hence G_{lm} should be zero. Then the scalar potential inside (V_{inside}) is given by

$$V(r,\theta,\phi) = \sum_{l=0}^{l=\infty} \sum_{m=-l}^{m=l} \big(F_{lm} r^{l}\big) Y_{lm}(\theta,\phi) \tag{2.20}$$

The other condition is that, as r increases to infinity the scalar potential should go to zero and the value of F_{lm} should be zero. And the scalar potential outside ($V_{outside}$) the sphere is given by

$$V(r,\theta,\phi) = \sum_{l=0}^{l=\infty} \sum_{m=-l}^{m=l} \big(G_{lm} r^{-(l+1)}\big) Y_{lm}(\theta,\phi) \tag{2.21}$$

The first boundary condition requires that the gradient of the potentials (the inside and outside) at the boundary surface of the sphere should be the same or be continuous: And that means: $V_{inside} = V_{outside}$ and that is

$$\sum_{l=0}^{l=\infty}\sum_{m=-l}^{m=l}\left(F_{lm}r^{l}\right)Y_{lm}(\theta,\phi)=\sum_{l=0}^{l=\infty}\sum_{m=-l}^{m=l}\left(G_{lm}r^{-(l+1)}\right)Y_{lm}(\theta,\phi) \tag{2.22}$$

Hence we get that $G_{lm}=F_{lm}r_0^{2l+1}$ where r_0 is the radius of the sphere for each value of l and m.

The second condition is that the normal components of the current densities (the inside and outside normal current density values) should be the same (continuous) at the boundary of the sphere and that is at $r=r_0$. We assumed that the conductivity inside the sphere is σ_s and outside the sphere or in the air is $\sigma=0$. From Ohm's law it is noted that the current density is given by $J=\sigma E$. Therefore the normal component of the current density inside the sphere that is J_{inside} is given by [36].

$$J_{inside}=(\sigma+j\omega\epsilon_s)\left(j\omega A\bullet\hat{r}+\sum_{l=0}^{l=\infty}\sum_{m=-l}^{m=l}lF_{lm}r^{l-1}Y_{lm}(\theta,\phi)\right) \tag{2.23}$$

And the normal component of the current density outside the sphere that is $J_{outside}$ is given by

$$J_{outside}=(j\omega\epsilon_0)\left(j\omega A\bullet\hat{r}+\sum_{l=0}^{l=\infty}\sum_{m=-l}^{m=l}(l+1)G_{lm}r^{l-1}Y_{lm}(\theta,\phi)\right) \tag{2.24}$$

The two current densities are the same (or continuous) means at the boundary surface i.e where $r=r_0$ we equate (2.23) and (2.24) as follows:

$$\begin{aligned}(\sigma+j\omega\epsilon_s)\left(j\omega A\bullet\hat{r}+\sum_{l=0}^{l=\infty}\sum_{m=-l}^{m=l}lF_{lm}r^{l-1}Y_{lm}(\theta,\phi)\right)=\\ (j\omega\epsilon_0)\left(j\omega A\bullet\hat{r}+\sum_{l=0}^{l=\infty}\sum_{m=-l}^{m=l}(l+1)G_{lm}r^{l-1}Y_{lm}(\theta,\phi)\right)\end{aligned} \tag{2.25}$$

Substituting equation $G_{lm}=F_{lm}{r_0}^{2l+1}$ into the above equation (2.25) eliminates the G_{lm} and then after carrying out some rearrangements and collection of like terms we get the equation

$$\begin{aligned}\sum_{l=0}^{l=\infty}\sum_{m=-l}^{m=l}\left(l(\sigma_s+j\omega\epsilon_s)+j\omega\epsilon_0(l+1)\right))F_{lm}r^{l-1}Y_{lm}(\theta,\phi)=\\ -\left(\sigma_s+j\omega(\epsilon_s-\epsilon_0)\right)j\omega A\bullet\hat{r}\end{aligned} \tag{2.26}$$

Next we need to determine the values of F_{lm} in the above equation (2.26). One way of doing this is multiply both sides of the equation (2.26) by orthogonal spherical harmonics and do a surface integral over the sphere surface. In addition, the computation of the vector potential A from equation (2) is also required. But this method is slow and relatively difficult to perform.

A rather easy and quicker method to compute the complex constants F_{lm} is to start from equation (2.2) and no need to multiply both sides of equation (2.26) by orthogonal spherical harmonics. In equation (2.2) the expression of the inverse distance $\frac{1}{|r-r'|}$ for which $r' > r$ can be written in terms of spherical harmonic functions as follows [37].

$$\frac{1}{|r-r'|} = 4\pi \sum_{l=0}^{\infty} \sum_{m=-l}^{m=l} \frac{1}{(2l+l)} \left(\frac{r^l}{r'^{l+1}} \right) {Y_{lm}}^*(\theta', \phi') Y_{lm}(\theta, \phi) \tag{2.27}$$

Inserting equation (2.27) for which r' is greater than r, into equation (2.2) and then performing some arrangements will yield the relation

$$\vec{A} = \mu I \sum_{l=0}^{\infty} \sum_{m=-l}^{m=l} r^l Y_{lm}(\theta, \phi) \left[\oint_{coil} \frac{Y^*_{lm}(\theta', \phi')}{(2l+l) r'^{l+1}} dl' \right] \tag{2.28}$$

The integral expression in the square bracket is a set of complex vector constants representing a given stimulating coil placement and shape. If we symbolize this set of complex vector constants by the letter C_{lm}, then equation (2.28) can be rewritten as

$$\vec{A} = \mu_0 I \sum_{l=0}^{l=\infty} \sum_{m=-l}^{m=l} r^l Y_{lm} C_{lm} \tag{2.29}$$

Once the scalar potential V and the vector potential $\vec{A}$ are determined in the spherical volume conductor, then the electric field $\vec{E}$ can be determined at any point inside the sphere using equation (2.11). And this is a relatively simpler and quicker method of computing the induced electric field inside the head due to an arbitrary stimulator coil shape and placement.

2.5 Application of the Calculated Induced Electric Field

The computation of the electric field in the sphere due to a nearby arbitrary and closed current coil at any required point of interest in the sphere has very useful clinical application during the process of TMS and MEG imaging of the brain.

2.5.1 Application to TMS

As pointed out earlier electromagnetic fields are being used clinically for diagnostics and treatment of several brain abnormalities or diseases. And TMS is a mechanism used to stimulate certain required brain tissues to treat brain disorders such as depression by repeated and successive stimulation of the affected neurons in the brain. When the electric field is induced and focused at the required spot, an electric current density (eddy current) will be induced at the same spot. It is this current which is responsible to stimulate the neurons and help restore normal functionality of the brain tissues for the good. In the process of stimulation only

the specific and affected area should be stimulated. However, the task of focusing the induced electric field only at the problematic location has been a challenge for the physicians.

After determining the coefficients F_{lm} in (2.26) and using the above equations (2.29) and also (2.20), the electric field can be computed easily and quickly using (2.11) on a personal computer for any type of coil shape and placement near the scalp. And this knowledge of the distribution of the electric field helps to solve the focusing problem during TMS.

Once we are able to compute the electric field distribution at any point of interest in the sphere (head), then the stimulating current density at the specific nerve location can be obtained by using ohm's law relation $\vec{J} = \sigma_s \vec{E}$ [38]. To administer TMS in the CNS, the specific structural location of the brain to be stimulated is best identified by using functional MRI of the brain.

2.5.2 Application to Magnetoencephalography (MEG)

The brain has tiny electrical ion currents that flow in and around membranes of its neurons during its communication activities. And by Fadaday's law of induction a corresponding tiny magnetic field is generated. This field can be detected around the scalp of the head using MEG machine. Magneto encephalography (MEG) is a technique of measuring such a tiny magnetic fields generated by the brain's electrical activities. The generated magnetic field of the brain is so small that can be as small as 10^{-12}Tesla.

The MEG machine has a sensitivity as small as 10^{-15}Tesla and so can detect the tiny fields and then locate the position of the sources of currents in the brain. The MEG is able to detect and measure the very tiny magnetic field of the brain because of its highly sensitive superconducting measuring device (which is cooled to nearly the absolute zero) called SQUID. The SQUID is placed in a shielded room in order to make the measurement of the field free from interfering nearby electric or magnetic fields.

Localization and recording (mapping) of the current sources in the brain is used to study how the normal brain functions and also helps to explore issues associated with brain pathology[1]. In this regard, the other application of easier and quicker computation of the distribution of the electric field and the current density inside the sphere (head) is that, the induced electric field can be used to interpret the magnetoencephalograms of the MEG. Magnetoencephalograms of the MEG are readings or recordings of the magnetic field of the brain by the MEG machine. Because of the reciprocity theorem the computed induced electric field can be used to represent the lead field of the MEG.

It is the reciprocity theorem that helps to relate the lead field of the MEG machine with the induced electric field in the brain. According to the the theory, there is a relationship between the current dipole P in the brain and the magnetic flux ϕ passing through the pick up coil of the SQUID[2] magnetometer near the scalp. The relation is given by

[1]Pathology is the study of disease

[2] SQUID is for **S**uperconducting **QU**antum **I**nterference **D**evice

$$\vec{\phi} = \frac{P \cdot \vec{E}(r)}{j\omega I}, \tag{2.30}$$

where
$\vec{E}(r)$ is the induced electric field in the brain during TMS and which we need to compute, P is the current dipole moment and r is the location of the dipole in the sphere measured from an appropriate reference point.

CHAPTER 3
EM FIELDS DUE TO Z GRADIENT FIELD SWITCHING IN MRI

3.1 Introduction

The analytic determination of the distribution of induced electric field and current density from arbitrary coil current in a nearby spherical homogeneous volume conductor was reviewed in the previous chapter.

Determination of the electric field anywhere in the model sphere was very essential to help focus the electric field strength at the required brain area for TMS. Harry A. C. Eaton did develop a mathematical model that enables us to compute the electric field and current density in the spherical volume conductor relatively easily and quickly by employing a set of line integrals along the excitation closed current coil of arbitrary shape [36]. The time taking and difficult way of computing the electric field involved surface integral and multiplication by orthogonal spherical harmonics.

The induced eddy current density in the brain helps to stimulate the neurons in the required and specific brain location. That was how a certain part of the brain was stimulated magnetically in the clinical applications of TMS for the purpose of treatment of some brain problems as well as for brain research.

In this chapter the analytic determination of the distribution of induced magnetic and electric fields, as well as the eddy current in a solid cylindrical volume conductor will be treated. The excitation current comes from a model of an actual MRI Z gradient coil current that has a time harmonic variation. The solid cylinder which is placed inside the gradient coil is taken as a model representing an actual whole human body or part of it undergoing an MRI scan. In addition the possible magnetic peripheral nerve stimulation on the surface of the human body due to the induced eddy currents will be examined.

3.2 Theory

In MRI, the gradient fields are primarily used for the purpose of spatially encoding the MRI signal and thereby help the selection of a slice of the body part to be imaged. In addition, during image acquisition, the current in the gradient coils is switched on and off very quickly for the purpose of better image resolution.

The frequently switching on and off of the current is accompanied by the induction of variable magnetic field. By Faraday's law the variable magnetic field induces electric field and the electric field in turn gives rise to formation of eddy currents in a conducting medium (the human body in this case). There is a concern that the induced eddy current may have a harmful interaction with the biological system and consequently cause undesired effects on the body.

Whether it is for safety or for deliberate medical treatment procedure, such as magnetic stimulation of the human body, it is essential to know the distribution of the electromagnetic fields in a human body induced by different nearby variable current carrying coils in devices may be at home or at working places.

Here the induced electric and magnetic fields distribution due to MRI Z gradient fields in a solid cylindrical volume conductor will be explored analytically by employing the vector potential caused by the current in the gradient coils. The current in the coils is assumed to vary at the typical MRI gradient frequency value of 3KHz.

3.3 Modelling and Parametric Assumptions

A solid conducting cylinder having infinite length and finite radius or thickness has been chosen to represent the whole human body undergoing an actual MRI scan. The solid cylinder model can also represent several parts of the human body such as the torso, the limbs, and even the nerve axons.

The model has also been assumed to be isotropic, homogeneous, possessing constant conductivity σ, and constant magnetic permeability $\vec{\mu}$. The current in the coil is assumed to be time harmonic which varies at low frequency $\frac{\vec{\omega}}{2\pi}$ (i.e as the function of $e^{i\omega t}$) to satisfy the quasi-static assumption. Because the frequency of the current is low, and the conductivity is assumed to be, such that $\sigma \gg \epsilon\omega$, the displacement current $\frac{\partial \vec{D}}{\partial t}$ in Ampere's law, is assumed to be very small than the conduction current, and hence it has been neglected. The low frequency of the exciting current also renders the propagation effect to be neglected. However, the skin depth which is given by $\delta = \sqrt{\frac{2}{\omega\mu\sigma}}$ can not be ignored for such intermediate frequency value.

Since the problem has a cylindrical symmetry, a cylindrical coordinate system is used. The problem is illustrated figuratively in Fig 3.1.

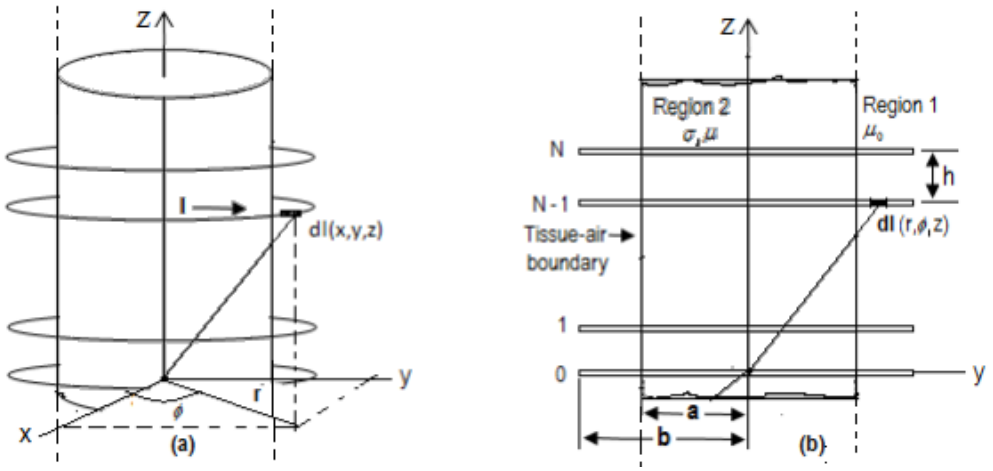

Figure 3.1: Schematic diagram of a solid cylinder with MRI z gradient coils around

All the coils are assumed to be connected in series. As a result, the excitation current in the loops does not vary with the azimuthal angle ϕ.

From Fig 3.1 we see that the radius of the cylinder is "a" and the radius of the gradient coil is "b". The coils have a spacing "h" between them. There are totally "N" number of coils. Region "1", is the insulating air surrounding the cylinder

(that is the space between the cylinder and the gradient coil) and region "2" is the solid cylindrical volume conductor (representing the tissue or the body).

3.4 Derivation of the EM Field Equations

3.4.1 Magnetic Vector Potential

As shown in Fig 3.1(b), a tiny current element of the coil $I\vec{dl}$ (a vector) is located at (r,ϕ,z) in the cylindrical coordinate system. The tiny coil element carries a current "I = I(t)" that is time harmonic and flowing at low (quasi-static) frequency in the coil. The coils are connected in series and hence each one of the N coils carries the same amount of current.

The current pulse in the Z gradient coil produces a magnetic vector potential all around the vicinity of the coil. And from the magnetic vector potential it is possible to compute the magnetic and electric field vectors by modifying the relevant Maxwell's equations for the quasi-static situation. Eddy currents will be induced in the cylindrical volume conductor because of the induced electric field which is caused by the time varying magnetic field. Once we get the induced electric field we can determine the eddy current density distribution in the cylindrical volume conductor using Ohm's law $\vec{J} = \sigma\vec{E}$.

The Z gradient coil current I, generates a vector potential $\vec{A_1}$ in the non-conducting region 1 (air - for which $a < r < b$) and a vector potential $\vec{A_2}$ in the conducting region 2 (cylinder - for which $0 \leq r \leq a$). Region 1 or the air has no charge density and its conductivity is zero. Hence it should satisfy Laplace's equation. Region 2 or the cylinder is a conductor and has a charge density and hence should satisfy Poisson's equation.

Now let us first proceed to compute the vector potentials $\vec{A_1}$ and $\vec{A_2}$ in the two regions. For regions 1 and 2, the Laplace's and Poisson's equations pertaining to the vector potentials $\vec{A_1}$ and $\vec{A_2}$ can be written respectively as follows

$$\nabla^2\vec{A_1} = 0 \tag{3.1}$$

$$\nabla^2\vec{A_2} = \mu\sigma\frac{\partial\vec{A_2}}{\partial t} \tag{3.2}$$

In the chosen cylindrical coordinate system, for Z gradient coil, the vector potential components $\vec{A}_{1,z}$, $\vec{A}_{2,z}$, $\vec{A}_{1,r}$ and $\vec{A}_{2,r}$ are all zero because of coil symmetry. And for this case of z gradient coil, the electric scalar potential V is zero and hence the induced electric field can be determined from the rate of change of the vector potential i.e from $\dfrac{\partial\vec{A}}{\partial t}$ [39].

In addition the vector potential components, $\vec{A}_{1,\phi}$ and $\vec{A}_{2,\phi}$ are independent of the angle ϕ because of rotational symmetry. Considering the aforementioned conditions, $\vec{A_1}$ and $\vec{A_2}$ can be expressed in the frequency domain as

$$\vec{A_1}(r,z,t) = \vec{A}_{1,\phi}(r,z)e^{j\omega t}\hat{\phi} \tag{3.3}$$

$$\vec{A_2}(r,z,t) = \vec{A}_{2,\phi}(r,z)e^{j\omega t}\hat{\phi} \tag{3.4}$$

Substituting equations (3.3) and (3.4) into (3.1) and (3.2) respectively, and performing the Laplacian operator in cylindrical coordinates yields the following expanded Laplace and Poisson's partial differential equations

$$\frac{\partial^2 \vec{A}_{1,\phi}}{\partial r^2} + \frac{1}{r}\frac{\partial \vec{A}_{1,\phi}}{\partial r} - \frac{\vec{A}_{1,\phi}}{r^2} + \frac{\partial^2 \vec{A}_{1,\phi}}{\partial z^2} = 0 \tag{3.5}$$

$$\frac{\partial^2 \vec{A}_{2,\phi}}{\partial r^2} + \frac{1}{r}\frac{\partial \vec{A}_{2,\phi}}{\partial r} - \frac{\vec{A}_{2,\phi}}{r^2} + \frac{\partial^2 \vec{A}_{2,\phi}}{\partial z^2} = jp^2 \vec{A}_{2,\phi}, \tag{3.6}$$

with

$$p^2 = \omega\mu\sigma \tag{3.7}$$

The vector potential $\vec{A}_{1,\phi}(r,z)$ in region 1 comes from two current sources. One current source is the time harmonic excitation current pulse flowing in the gradient coil and it is denoted by $\vec{A}'_{1,\phi}(r,z)$. The second current source is the induced eddy current caused by the varying magnetic field in the cylinder and it is denoted by $\vec{A}''_{1,\phi}(r,z)$.

Hence the total vector potential in region 1, as a sum of two potentials from two different current sources is written as

$$\vec{A}_{1,\phi}(r,z) = \vec{A}'_{1,\phi}(r,z) + \vec{A}''_{1,\phi}(r,z) \tag{3.8}$$

Starting from Biot - Savart law, the magnetic vector potential $\vec{A}'_{1,\phi}(r,z)$ in region 1 (air and unbounded region), due to a single excitation coil of radius 'a' which is carrying a time harmonic current I(t), in the cylindrical coordinate system, is given by [40].

$$\vec{A}'_{1,\phi}(r,z) = \frac{\mu a I}{2\pi}\int_0^{\pi} \frac{cos\phi\, d\phi}{\sqrt{a^2 + r^2 + z^2 - 2arcos\phi}} \tag{3.9}$$

The above integral constitutes an integration of elliptic integrals which has its own closed form solution. To find these solutions we have to make a variable change as follows and proceed. That is, let

$$\phi = \pi - 2\theta, \tag{3.10}$$

and

$$d\phi = -2d\theta, \tag{3.11}$$

Next

$$cos(\phi) = cos(\pi - 2\theta), \tag{3.12}$$

$$cos(\phi) = cos(2\theta - \pi), \tag{3.13}$$

$$cos(\phi) = -cos(2\theta) \tag{3.14}$$

Then we have

$$cos(\phi) = 2sin^2\theta - 1 \tag{3.15}$$

Substituting equations (3.11) and (3.15) in equation (3.9) we get

$$\vec{A'}_{1,\phi}(r,z) = \frac{\mu a I}{2\pi}\int_{\frac{\pi}{2}}^{0} \frac{(2sin^2\theta - 1)(-2d\theta)}{\sqrt{a^2 + r^2 + z^2 - 2ar(2sin^2\theta - 1)}} \tag{3.16}$$

$$\vec{A'}_{1,\phi}(r,z) = \frac{\mu a I}{\pi}\int_{0}^{\frac{\pi}{2}} \frac{(2sin^2\theta - 1)d\theta}{\sqrt{a^2 + r^2 + z^2 + 2ar - 4rasin^2\theta}} \tag{3.17}$$

As the integrand is an even function, the range of integration is reduced by half and the whole integrand is multiplied by two for compensation. Since the integration is with respect to θ, we can factor out some variables that are constant and make the following rearrangement

$$\vec{A'}_{1,\phi}(r,z) = \frac{\mu a I}{\pi\sqrt{z^2 + (a+r)^2}}\int_{0}^{\frac{\pi}{2}} \frac{(2sin^2\theta - 1)d\theta}{\sqrt{1 - \frac{4rasin^2\theta}{z^2+(a+r)^2}}} \tag{3.18}$$

Then we make the following substitution

$$k^2 = \frac{4ra}{z^2 + (a+r)^2} \tag{3.19}$$

Then using the above value of k^2 we get

$$\vec{A'}_{1,\phi}(r,z) = \frac{\mu k I}{2\pi}\sqrt{\frac{a}{r}}\int_{0}^{\frac{\pi}{2}} \frac{(2sin^2\theta - 1)d\theta}{\sqrt{1 - k^2sin^2\theta}} \tag{3.20}$$

To simplify the expression we make another substitution such that

$$\sigma = \frac{\mu k I}{2\pi}\sqrt{\frac{a}{r}} \tag{3.21}$$

Then we get

$$\vec{A'}_{1,\phi}(r,z) = \sigma\int_{0}^{\frac{\pi}{2}} \frac{(2sin^2\theta - 1)d\theta}{\sqrt{1 - k^2sin^2\theta}} \tag{3.22}$$

Splitting equation (3.22) we get

$$\vec{A'}_{1,\phi}(r,z) = 2\sigma\int_{0}^{\frac{\pi}{2}} \frac{sin^2\theta d\theta}{\sqrt{1 - k^2sin^2\theta}} - \sigma\int_{0}^{\frac{\pi}{2}} \frac{d\theta}{\sqrt{1 - k^2sin^2\theta}} \tag{3.23}$$

Multiplying the first term in (3.23) by $\frac{k^2}{k^2}$ we can write as

$$\vec{A'}_{1,\phi}(r,z) = \frac{2\sigma}{k^2}\int_{0}^{\frac{\pi}{2}} \frac{k^2sin^2\theta d\theta}{\sqrt{1 - k^2sin^2\theta}} - \sigma\int_{0}^{\frac{\pi}{2}} \frac{d\theta}{\sqrt{1 - k^2sin^2\theta}} \tag{3.24}$$

Next subtracting and then adding $\left(\frac{1-k^2sin^2\theta}{\sqrt{1-k^2sin^2\theta}}\right)$, to the first term in (3.24) and

rearranging yields,

$$\vec{A}'_{1,\phi}(r,z) = \frac{2\sigma}{k^2}\int_0^{\frac{\pi}{2}} \left(\frac{d\theta}{\sqrt{1-k^2sin^2\theta}}\right) - \frac{2\sigma}{k^2}\int_0^{\frac{\pi}{2}} \left(\frac{1-k^2sin^2\theta}{\sqrt{1-k^2sin^2\theta}}\right) d\theta - \sigma\int_0^{\frac{\pi}{2}} \left(\frac{d\theta}{\sqrt{1-k^2sin^2\theta}}\right) \quad (3.25)$$

and then

$$\vec{A}'_{1,\phi}(r,z) = \frac{2\sigma}{k^2}\int_0^{\frac{\pi}{2}} \left(\frac{d\theta}{\sqrt{1-k^2sin^2\theta}}\right) - \frac{2\sigma}{k^2}\int_0^{\frac{\pi}{2}} \left(\sqrt{1-k^2sin^2\theta}\right) - \sigma\int_0^{\frac{\pi}{2}} \left(\frac{d\theta}{\sqrt{1-k^2sin^2\theta}}\right) \quad (3.26)$$

The complete elliptic integrals of the first $K(k)$ and second $E(k)$ kind, of which the upper limit is $\frac{\pi}{2}$ are defined respectively by [41].

$$K(k) = \int_0^{\frac{\pi}{2}} \frac{d\theta}{\sqrt{1-k^2sin^\theta}} \quad (3.27)$$

and

$$E(k) = \int_0^{\frac{\pi}{2}} \sqrt{1-k^2sin^\theta}d\theta \quad (3.28)$$

If we make the substitution of the elliptic integrals we get

$$\vec{A}'_{1,\phi}(r,z) = \frac{2\sigma}{k^2}K(k) - \frac{2\sigma}{k^2}E(k) - \sigma K(k) \quad (3.29)$$

$$\vec{A}'_{1,\phi}(r,z) = \frac{\sigma}{k^2}\left[2K(k) - k^2K(k) - 2E(k)\right] \quad (3.30)$$

Next we shall substitute the value of $\sigma = \frac{\mu kI}{2\pi}\sqrt{\frac{a}{r}}$ and rearrange as follows

$$\vec{A}'_{1,\phi}(r,z) = \frac{\mu I}{2\pi k}\sqrt{\frac{a}{r}}\left[2K(k) - k^2K(k) - 2E(k)\right] \quad (3.31)$$

$$\vec{A}'_{1,\phi}(r,z) = \frac{\mu aI}{2\pi k\sqrt{ar}}\left[2K(k) - k^2K(k) - 2E(k)\right] \quad (3.32)$$

$$\vec{A}'_{1,\phi}(r,z) = \frac{\mu aI}{\pi}\left((\frac{1}{2k\sqrt{ar}})\left[2K(k) - k^2K(k) - 2E(k)\right]\right) \quad (3.33)$$

The expression with in the larger round brackets of equation (3.33) which contains the sum of the complete elliptic integral is equal to the infinite integral expression of the product of the modified Bessel functions of the first and second kind as given below [42].

$$(\frac{1}{2k\sqrt{ar}})\left[2K(k) - k^2K(k) - 2E(k)\right] = \int_0^\infty K_1(kr)I_1(ka)cosk(z)dk \quad (3.34)$$

And hence the final expression for the magnetic vector potential due to the excitation coil, in terms of the modified Bessel functions will be

$$\vec{A'}_{1,\phi}(r,z) = \frac{\mu a I}{\pi}\int_0^\infty K_1(kr)I_1(ka)cosk(z)dk \tag{3.35}$$

And for any other single i^{th} loop the vector potential becomes [40]

$$\vec{A'}_{1,\phi}(r,z) = \frac{\mu a I}{\pi}\int_0^\infty K_1(kr)I_1(ka)cosk(z-ih)dk \tag{3.36}$$

We note that the I_1 and K_1 are modified Bessel functions of the first and second kind.

The other vector potential $\vec{A''}_{1,\phi}(r,z)$ due to the eddy current induced in the cylinder, at the same site of region 1 (that is air) has a similar expression given by the relation

$$\vec{A''}_{1,\phi}(r,z) = \sum_i^N \int_0^\infty C_i(k)K_1(kr)cosk(z-ih)dk \tag{3.37}$$

The constant $C_i(k)$ comes from applying the boundary condition at the air - cylinder surface, where the condition is that the parallel component of the vector potential field is continuous. Then the total vector potential in the air is the sum of the vector potentials in equations (3.36) and (3.37) and is given by

$$\vec{A}_{1,\phi}(r,z) = \frac{\mu a I}{\pi}\sum_{i=0}^N \int_0^\infty K_1(kr)I_1(ka)cosk(z-ih)dk + \sum_{i=0}^N \int_0^\infty C_i(k)K_1(kr)cosk(z-ih)dk \tag{3.38}$$

The vector potential in the cylinder (region 2) is only due to the excitation z gradient coil current. It is obtained by solving the Poisson's equation expressed in equation (3.6). This equation has the r and z variables coupled in it. Therefore, to solve for $\vec{A}_2(r,z)$ we need to use the technique of separation of variables to split the equation into two independent equations.

Assuming that $\vec{A}_2(r,z)$ is equal to the product of the two independent functions R=R(r) and Z=Z(z), we can write $\vec{A}_2(r,z) = R(r) \times Z(z)$. When substituting this product solution in equation (3.6), we get

$$\frac{\partial^2 R(r)Z(z)}{\partial r^2} + \frac{1}{r}\frac{\partial R(r)Z(z)}{\partial r} - \frac{R(r)Z(z)}{r^2} + \frac{\partial^2 R(r)Z(z)}{\partial z^2} = jp^2 R(r)Z(z) \tag{3.39}$$

After dividing both sides of the above equation by R(r)Z(z) and rearranging

we get

$$\frac{1}{R(r)}\frac{\partial^2 R(r)}{\partial r^2}+\frac{1}{R(r)}\frac{1}{r}\frac{\partial R(r)}{\partial r}-\frac{1}{r^2}+\frac{1}{Z(z)}\frac{\partial^2 Z(z)}{\partial z^2}-jp^2=0 \tag{3.40}$$

On the left side of equation (3.40) the first three terms depend on r. We can take the remaining terms as being dependent on z. For the sum of the two independent equations to be zero, each must be equal to the same but opposite separation constant number. Choosing λ^2 as a separation constant the two equations will be expressed as

$$\frac{1}{R(r)}\frac{\partial^2 R(r)}{\partial r^2}+\frac{1}{R(r)}\frac{1}{r}\frac{\partial R(r)}{\partial r}-\frac{1}{r^2}=\lambda^2 \tag{3.41}$$

And

$$\frac{1}{Z(z)}\frac{\partial^2 Z(z)}{\partial z^2}-jp^2=-\lambda^2 \tag{3.42}$$

Next we proceed to solve these two equations one by one. First, we solve equation (3.42) by rearranging it as follows

$$\frac{\partial^2 Z(z)}{\partial z^2}-Z(z)jp^2+Z(z)\lambda^2=0 \tag{3.43}$$

$$\frac{\partial^2 Z(z),i}{\partial z^2}+Z(z),i\left(\lambda^2-jp^2\right)=0 \tag{3.44}$$

The number i= 0,1,2,...,N; which is a non negative integer, is the number of coils. The expression in the bracket that is (λ^2–jp^2) has been replaced by a continuous variable k^2 such that $k^2=\lambda^2$–jp^2. With the symbol i omitted for visual clarity we have

$$\frac{d^2 Z(z)}{dz^2}+k^2 Z(z)=0 \tag{3.45}$$

Equation (3.45) is an ODE of the second order and has a general solution given as

$$Z(z)=Asink(z)+Bcosk(z) \tag{3.46}$$

However, using a trigonometric identity that transforms equation (3.46) into a single cosine function, the solution for one of the z-gradient coils can be written as [35].

$$Z(z)\approx cosk(z-ih) \tag{3.47}$$

Next we solve equation (3.41) as follows

$$\frac{1}{R(r)}\frac{\partial^2 R(r)}{\partial r^2}+\frac{1}{R(r)}\frac{1}{r}\frac{\partial R(r)}{\partial r}-\frac{1}{r^2}-\lambda^2=0 \tag{3.48}$$

After multiplying (3.48) by R(r) and doing some rearrangement we get

$$\frac{d^2 R(r)}{dr^2}+\frac{1}{r}\frac{dR(r)}{dr}-\left(\frac{1}{r^2}+\lambda^2\right)R(r)=0 \tag{3.49}$$

And this equation (3.49) has the form of the standard modified Bessel equation

which will have real valued solutions called modified Bessel functions $I_n(\lambda r)$ and $K_n(\lambda r)$ and they are of the first and second kind respectively.

Hence the general solutions of equation (3.49) can be written as

$$R(r) = D_i(k)I_n(\lambda r) + E_i(k)K_n(\lambda r) \tag{3.50}$$

Since the Bessel function of the second kind '$K_n(\lambda r)$' decays inside the cylinder as a function of 'r', it is not useful as a solution in this case and only the '$I_n(\lambda r)$' Bessel functions are taken as a solution in region 2 (in the cylinder) and so the solution to (3.49) will be reduced to

$$R(r) = D_i(k)I_n(\lambda r) \tag{3.51}$$

Finally the general solution of the vector potential expressed in the Poisson's equation (3.6) in the cylinder will be the product of the solutions (3.47) for the z component and the solution (3.51) for the r component. Then for the i^{th} single coil we can write the solution of the vector potential in the cylinder as

$$\vec{A}_{2,\phi}(r,z) = R(r)Z(z) \tag{3.52}$$

Or

$$\vec{A}_{2,\phi}(r,z) = \int_0^\infty D_i(k)I_1(\lambda r)cosk(z-ih) \tag{3.53}$$

For all the coils from i = 0 to N, we take the contribution from each coil and apply the superposition principle and take the sum to obtain the following expression for $\vec{A}_{2,\phi}(r,z)$ as

$$\boxed{\vec{A}_{2,\phi}(r,z) = \sum_i^N \int_0^\infty D_i(k)I_1(\lambda r)cosk(z-ih)} \tag{3.54}$$

The constants C_i, and D_i, can be determined by applying the boundary condition at the air-cylinder (air-tissue interface) interface. The required condition is that the vector potential fields should be continuous where the radial distance is equal to the cylinder radius, that is $r = a$. After the application of the boundary condition the constants C_i, and D_i are found to be [40].

$$C_i(k) = \frac{\mu a I}{\pi}\frac{K_1(ka)[kI_0(kb)I_1(\lambda b) - \lambda I_0(\lambda b)I_1(kb)]}{M}, \tag{3.55}$$

and

$$D_i(k) = \frac{\mu a I}{\pi b}\frac{K_1(ka)}{M}, \tag{3.56}$$

where

$$M = kK_0(kb)I_1(\lambda b) + \lambda I_0(\lambda b)K_1(kb) \tag{3.57}$$

3.4.2 Magnetic Field Equations in Regions One and Two

Once we get the vector potentials in the two regions, we can get the respective magnetic field components in both regions using the curl relation $\vec{B} = \vec{\nabla} \times \vec{A}$.

The vector potential has only one component along the direction of the current and that is in the ϕ direction but the corresponding magnetic fields have two components which are in the radial (r) and the axial (z) directions in each region.

Accordingly, the magnetic field components $\vec{B}_r$ and $\vec{B}_z$ for each region 1 and 2 are calculated by taking the partial derivatives of the vector potential with respect to the r and z as follows

(i) In region one

(a) r component of $\vec{B}_1$

$$\vec{B}_{1,r}(r,z) = \vec{\nabla}\times\vec{A}_{1,\phi} = -\frac{\partial\vec{A}_{1,\phi}}{\partial z} \tag{3.58}$$

Therefore substituting $\vec{A}_{1,\phi}$ from (3.38) into equation (3.58) we get

$$\vec{B}_{1,r}(r,z) = -\sum_{i=0}^{N}\int_0^\infty \frac{\partial}{\partial z}\left(C_i(k)K_1(kr)cosk(z-ih)dk\right) - \sum_{i=0}^{N}\int_0^\infty \frac{\partial}{\partial z}\left(\frac{\mu aI}{\pi}K_1(ka)I_1(kr)cosk(z-ih)dk\right) \tag{3.59}$$

And after performing the derivative the radial component of $\vec{B}_1$ will be

$$\vec{B}_{1,r}(r,z) = \sum_{i=0}^{N}\int_0^\infty (kC_i(k)K_1(kr)sink(z-ih)dk) + \sum_{i=0}^{N}\int_0^\infty \left(\frac{\mu aI}{\pi}kK_1(ka)I_1(kr)sink(z-ih)dk\right) \tag{3.60}$$

(b) z component of $\vec{B}_1$

$$\vec{B}_{1,z}(r,z) = \nabla\times\vec{A}_{1,\phi} = \frac{1}{r}\frac{\partial}{\partial r}(r\vec{A}_{1,\phi}), \tag{3.61}$$

and after carrying out the derivative, the axial component of the $\vec{B}_1$ will be

$$\vec{B}_{1,z}(r,z) = -\sum_{i=0}^{N}\int_0^\infty (kC_i(k)K_0(kr)cosk(z-ih)dk) + \sum_{i=0}^{N}\int_0^\infty \left(\frac{\mu aI}{\pi}kK_1(ka)I_0(kr)cosk(z-ih)dk\right) \tag{3.62}$$

(ii) In region two

(a) r component of $\vec{B}_2$

$$\vec{B}_{2,r}(r,z) = \vec{\nabla}\times\vec{A}_{2,\phi} = -\frac{\partial\vec{A}_{2,\phi}}{\partial z} \tag{3.63}$$

Substituting the formula for $\vec{A}_{2,\phi}$ we get

$$\vec{B}_{2,r}(r,z) = \sum_{i=0}^{N}\int_0^\infty -\frac{\partial}{\partial z}\left(D_1(k)I_1(\lambda r)cosk(z-ih)dk\right) \tag{3.64}$$

After carrying out the derivative the radial component of $\vec{B}_2$ will be

$$\boxed{\vec{B}_{2,r}(r,z) = \sum_{i=0}^{N}\int_0^\infty kD_1(k)I_1(\lambda r)sink(z-ih)dk} \tag{3.65}$$

(b) z component of $\vec{B}_2$

$$\vec{B}_{2,z}(r,z) = \vec{\nabla}\times\vec{A}_{2,\phi} = \frac{1}{r}\frac{\partial r\vec{A}_{2,\phi}}{\partial r} \tag{3.66}$$

Substituting for $\vec{A}_{2,\phi}$ and carrying out the derivative will yield the axial component of the $\vec{B}_2$ field as

$$\vec{B}_{2,z}(r,z) = \sum_{i=0}^{N}\int_0^\infty \lambda D_1(k)I_0(\lambda r)cosk(z-ih)dk \tag{3.67}$$

3.4.3 Electric Field Equation in the Cylinder

Taking the assumption that the vector potential is harmonic time dependent, that is $\vec{A}(\phi,t) = \vec{A}(\phi)e^{-j\omega t}$ the electric field distribution can be calculated from the partial differential equation that relates the vector potentials with the electric fields, which is

$$\vec{E} = -\frac{\partial\vec{A}(\phi,t)}{\partial t} = -j\omega\vec{A}(\phi) \tag{3.68}$$

Using the relationship in equation (3.68), the electric field in the cylinder (region 2) which is the main focus of this report is given by

$$\vec{E}_{2,\phi}(r,z) = -\frac{\partial\vec{A}_{2,\phi}(\phi,t)}{\partial t} \tag{3.69}$$

Substituting for $\vec{A}_{2,\phi}(\phi,t)$

$$\vec{E}_{2,\phi}(r,z) = -\frac{\partial}{\partial t}\left[\sum_{i=0}^{N}\int_0^\infty e^{-j\omega t}D_1(k)I_1(\lambda r)cosk(z-ih)dk\right] \tag{3.70}$$

Therefore the electric field distribution in the cylinder becomes

$$\boxed{\vec{E}_{2,\phi}(r,z) = -j\omega\sum_{i=0}^{N}\int_0^\infty D_1(k)I_1(\lambda r)cosk(z-ih)dk} \tag{3.71}$$

3.4.4 Eddy Current Equation in the Cylinder

It is the eddy current that is responsible for the stimulation of the peripheral nerve. The eddy current density due to the coil current in the cylindrical volume conductor varies based on the radial and axial distances 'r' and 'z' respectively.

However, the eddy current density, does not vary with the angle ϕ. That is because the loops are placed at the center of the cylinder about the z – axis, and also the excitation current does not vary along ϕ as the coils are connected in series. For the assumed isotropic medium, using the equation $i_\phi = \sigma E$, the eddy current density distribution inside the solid cylinder is given by

$$\boxed{i_\phi = \sigma \vec{E}_{2,\phi}(r,z) = -j\omega\sigma \sum_{i=0}^{N} \int_0^\infty D_1(k) I_1(\lambda r) cosk(z - ih) dk} \tag{3.72}$$

3.5 Application to Magnetic Peripheral Nerve Stimulation

3.5.1 The Peripheral Nervous System

Our nervous system is generally responsible for all sorts of bodily information communication that is taking place in our body both from all parts of the body to the brain and vice versa. This communication takes place by using electrical and chemical signals. Peripheral nerve system is one of the two major components of the nervous system. The peripheral nervous system is a huge network that includes all the nerves and neurons outside the brain and spinal cord [43]. Neurons are nerve cells in the nervous system which are specifically designed for executing communication in the body.

Any impulsive message such as pain or other internal and external stimulus is transmitted from the peripheral parts of the body to the spinal cord and to the brain by the so called sensory neurons. And any response from the brain to the other body parts for action to take place is transmitted by the motor neurons.

3.5.2 Application of the Fields to PNS

The knowledge of the distribution of the electric field and eddy currents induced in the model cylinder due to the Z gradient coils of MRI is necessary. This has an important application in predicting a possible incidence of peripheral nerve stimulation on the patient.

One thing is that, during MRI scanning, the frequency of the gradient fields should not be extreme to the extent of putting the patient at risk of experiencing unwanted nerve tissue stimulation which can be dangerous [44]. If the gradient field frequency is above the threshold frequency, the resulting nerve stimulation may be dangerous for health. Davids et al; have predicted the threshold frequency values for several body parts of a patient [45]. Also Reilly has presented a rational methodology for evaluating excitation thresholds for peripheral nerve stimulation [46].

The other thing is that peripheral nerve stimulation can be used clinically for the purpose of relieving pain or treatment of some nerve problems and even for healing wounds that may be chronic or slow healing caused by different factors [47]. Therefore, whether it is for safety issue or deliberate beneficial use, calculation of the induced eddy current that may be created due to a known gradient field frequency is essential to properly monitor PNS.

3.5.3 Mechanism of Magnetic Peripheral Nervous Stimulation

There is a magnetic nerve stimulator which is an electronic device that is constructed for the purpose of stimulating the nerve using magnetic field. Magnetic stimulation mechanism employs Faraday's law of electromagnetic induction. Using a coil in the device, a changing current induces a changing magnetic field and then the changing magnetic field creates an electric field and finally the electric field generates eddy currents in the required conducting medium such as a tissue or a nerve. It is this current that is used to stimulate or excite the nerve or the tissue.

The stimulator device consists of capacitors and an inductor. The inductor is the stimulating coil. Electric energy for stimulation is obtained from the charged capacitors which can reach as high as 4kV. When the capacitors are discharged for use, the high intensity current that may reach as high as 5kA passes through the coil generating very strong changing magnetic field that lasts for a very brief duration of time. The capacitor discharge is controlled by a thyristor switch that withstands the high current. The direction of the current flow in the coil or inductor is opposite to the direction of the induced eddy currents in the nerve tissue [48].

In our life it can happen that the normal communication between the sensory and motor neurons may fail or the nerve may physically be damaged or may also be painful due to several reasons. This nerve disorder can be caused from different factors such as from accidents on the body or from incidents associated with surgery. Several of the peripheral nerve disorders causing pain, nowadays, can be treated by peripheral magnetic nerve stimulation or magnetic excitation of the nerve administered several times to the affected nerve.

One of the several ways of exciting a nerve is adding charges directly into the nerve. The addition of charges into a nerve will increase the membrane potential of the nerve relative to the surrounding extra cellular fluid. The direct addition of charges into the required nerve can be achieved by the magnetically induced electric field if the right amount of the electric field and its proper orientation is known. Fig. 3.2 shows roughly how a certain nerve on the arm is stimulated by a single excitation coil.

When the membrane potential of the nerve exceeds the normal negative level, the nerve will be stimulated and the associated nerve disorder may be solved [49].

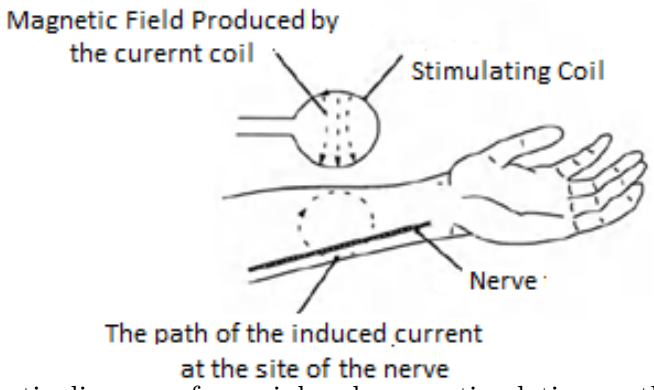

Figure 3.2: Schematic diagram of a peripheral nerve stimulation on the arm by a single coil

3.6 Field Plots

By now the solutions for the magnetic and electric fields as well as for the eddy current in the cylinder have been found as stated in equations (3.64), (3.70) and (3.71) respectively. In all the solutions the modified Bessel function of the first kind $I_1(\lambda r)$ is used. Next, by taking a first order asymptotic approximation of this first kind modified Bessel function, for large values of the argument $x = \lambda r$ the distributions of the fields and the eddy current density against the radial distance of the cylinder will be plotted to see how the fields behave in the cylinder.

Accordingly, the modified Bessel functions of the first and the second kind having order n and argument $x = \lambda r$, have an asymptotic series expansion approximations given as

$$I_n(x) = \frac{e^x}{\sqrt{2\pi x}}\left[1 - \frac{4n^2 - 1^2}{1(x)}\left(1 - \frac{(4n^2 - 3^2)}{2(x)}\left(1 - \frac{(4n^2 - 5^2)}{3(x)}(-...)\right)\right)\right] \quad (3.73)$$

For the case of this report, the argument x is equal to the product of the separation constant λ and the radial distance r from the axis of the cylinder and that is, $x = \lambda r$. Substituting the value of x and taking the first order n=1, the expansion becomes

$$I_1(\lambda r) = \frac{e^{\lambda r}}{\sqrt{2\pi\lambda r}}\left[1 - \frac{3}{1(8\lambda r)}\left(1 + \frac{5}{2(8\lambda r)}\left(1 + \frac{21}{3(\lambda r)}(1 + ...)\right)\right)\right] \quad (3.74)$$

Next if the first order approximation of $I_1(\lambda r)$ is taken, it becomes [50].

$$I_1(\lambda r) \propto \frac{e^{\lambda r}}{\sqrt{2\pi\lambda r}} \quad (3.75)$$

In the next sections a substitution of the this first order approximated expression of $I_1(\lambda r)$ will be made for analyzing the field equations further.

3.6.1 Magnetic Field Distribution in the Cylinder

As given in equation (3.39), the radial magnetic field distribution in the cylinder has been derived to be

$$\vec{B}_{2,r}(r,z) = \sum_{i=0}^{N}\int_0^{\infty} kD_i(k)I_1(\lambda r)sink(z-ih)dk \tag{3.76}$$

Making a substitution of the first order approximation of $I_1(\lambda r)$ gives

$$\vec{B}_{2,r}(r,z) = \sum_{i=0}^{N}\int_0^{\infty} kD_i(k)\left(\frac{e^{\lambda r}}{\sqrt{2\pi\lambda r}}\right)sink(z-ih)dk \tag{3.77}$$

Substitution in place of λ where $\lambda = \sqrt{k^2+jp^2}$ and $p^2 = \omega\mu\sigma$ yields

$$\vec{B}_{2,r}(r,z) = \sum_{i=0}^{N}\int_0^{\infty} kD_i(k)\left(\frac{e^{\left(\sqrt{k^2+jp^2}\right)r}}{\sqrt{2\pi(\sqrt{k^2+jp^2})r}}\right)sink(z-ih)dk \tag{3.78}$$

If the p^2 is factored out of the square roots the equation becomes

$$\vec{B}_{2,r}(r,z) = \sum_{i=0}^{N}\int_0^{\infty} kD_i(k)\left(\frac{e^{rp\left(\sqrt{\left(\frac{k}{p}\right)^2+j}\right)}}{\sqrt{2\pi pr\left(\sqrt{\left(\frac{k}{p}\right)^2+j}\right)}}\right)sink(z-ih)dk \tag{3.79}$$

As expressed previously $p = \sqrt{\omega\mu\sigma}$ and the skin depth is given by the relation $\delta = \dfrac{\sqrt{2}}{\sqrt{\omega\mu\sigma}}$. The skin depth, which is also called penetration depth, is the distance into the cylinder to which the current density falls to 37% of its strength at the surface of the cylinder. Skin depth is inversely dependent on the square root of the frequency of the induced field. We have that p and δ are related by $p = \dfrac{\sqrt{2}}{\delta}$. Substituting the value for p in the above equation yields

$$\vec{B}_{2,r}(r,z) = \left[\sum_{i=0}^{N}\int_0^{\infty} kD_i(k)\left(\frac{e^{\frac{r}{\delta}\left(\sqrt{2}\sqrt{\left(\frac{\delta k}{\sqrt{2}}\right)^2+j}\right)}}{\sqrt{\frac{2\pi r}{\delta}\left(\sqrt{2}\sqrt{\left(\frac{\delta k}{\sqrt{2}}\right)^2+j}\right)}}\right)sink(z-ih)dk\right] \tag{3.80}$$

For further simplification, let $a(k)$ be such that $a(k) = \left(\sqrt{2}\sqrt{\left(\frac{\delta k}{\sqrt{2}}\right)^2+j}\right)$. Then substituting $a(k)$ and rearranging yields

$$\vec{B}_{2,r}(r,z) = \sum_{i=0}^{N} \int_0^{\infty} kD_i(k) \left(\frac{e^{\left(\frac{r}{\delta}\right)a(k)}}{\sqrt{\frac{r}{\delta}}\sqrt{2\pi a(k)}} \right) sink(z-ih)dk \tag{3.81}$$

The need here is to explore the dependence of the magnetic field on the cylinder radius 'r'. Therefore, out of the whole expression for $\vec{B}_{2,r}$, in equation (3.80), for z=0, the dominant function is seen to be $\frac{e^{\frac{r}{\delta}}}{\sqrt{\frac{r}{\delta}}}$. Hence the magnetic field expression can be expressed as being proportional to the radius of the cylinder 'r' as follows

$$\vec{B}_{2,r}(r, z=0) \propto \frac{e^{\frac{r}{\delta}}}{\sqrt{\frac{r}{\delta}}} \tag{3.82}$$

Equation (3.81) shows that the magnetic field distribution in the cylinder depends on 'r' both exponentially and as well as on $\frac{1}{\sqrt{r}}$ and its ultimate behavior will be determined by the effective outcome.

3.6.2 Electric Field Distribution in the Cylinder

From equation (3.70) the electric field distribution in the cylinder has been derived to be

$$\vec{E}_{2,\phi}(r,z) = -j\omega \sum_{i=0}^{N} \int_0^{\infty} D_i(k) I_1(\lambda r) cosk(z-ih)dk \tag{3.83}$$

Making a substitution of the first order approximation of $I_1(\lambda r)$ yields

$$\vec{E}_{2,\phi}(r,z) = -j\omega \sum_{i=0}^{N} \int_0^{\infty} D_i(k) \left(\frac{e^{\lambda r}}{\sqrt{2\pi\lambda r}} \right) cosk(z-ih)dk \tag{3.84}$$

Substituting in place of λ where $\lambda = \sqrt{k^2 + jp^2}$ and $p^2 = \omega\mu\sigma$ and after doing some rearrangements the expression takes the form

$$\vec{E}_{2,\phi}(r,z) = -j\omega \sum_{i=0}^{N} \int_0^{\infty} D_i(k) \left(\frac{e^{\frac{r}{\delta}\left(\sqrt{2}\sqrt{\left(\frac{\delta k}{\sqrt{2}}\right)^2 + j}\right)}}{\sqrt{\frac{2\pi r}{\delta}\left(\sqrt{2}\sqrt{\left(\frac{\delta k}{\sqrt{2}}\right)^2 + j}\right)}} \right) cosk(z-ih)dk \tag{3.85}$$

For further simplification, we let $a(k) = \left(\sqrt{2}\sqrt{\left(\frac{\delta k}{\sqrt{2}}\right)^2 + j}\right)$. Then substituting $a(k)$ and rearranging we get

$$\vec{E}_{2,\phi}(r,z) = -j\omega \left[\sum_{i=0}^{N} \int_0^{\infty} D_i(k) \left(\frac{e^{\left(\frac{r}{\delta}\right)a(k)}}{\sqrt{\frac{r}{\delta}}\sqrt{2\pi a(k)}} \right) cosk(z-ih)dk \right] \tag{3.86}$$

As in the case for the magnetic field, here also what is explored is the depen-

dence of the electric field on the radius of the cylinder. Therefore, as can be seen in equation (3.85), for z=0, out of the whole expression for the electric field, the dominant function that depends on 'r' is $\frac{e^{\frac{r}{\delta}}}{\sqrt{\frac{r}{\delta}}}$. For the sake of seeing the electric field dependence on 'r', it is possible to approximate the electric field expression in the cylinder by the relation

$$\vec{E}_{2,\phi}\left(r, z=0\right) \propto \vec{\omega}\frac{e^{\frac{r}{\delta}}}{\sqrt{\frac{r}{\delta}}} \tag{3.87}$$

We see that the electric and the magnetic fields in the cylinder have similar pattern of dependence on 'r', except that the electric field is multiplied by the angular velocity $\vec{\omega}$, which means that the magnitude of the electric field is greater than the magnetic field. Next we will plot the electric field - as expressed by equation (3.87), against the radius of the cylinder. To do that we take some characteristics values

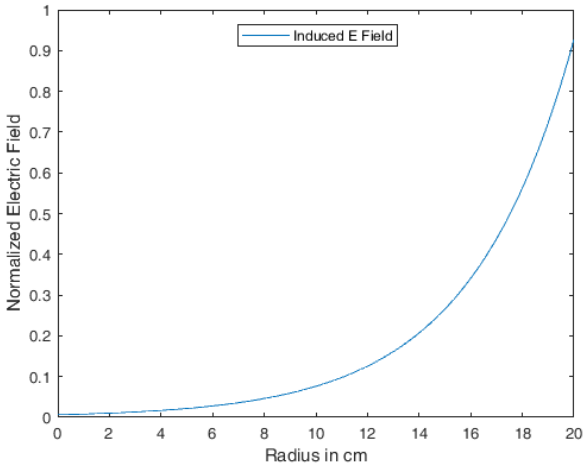

Figure 3.3: Electric Field distribution as a function of the radius of the cylinder

of the conducting cylinder, such as its conductivity (σ), magnetic permeability (μ) and the excitation current frequency (f), and then calculate the skin depth first. The solid cylinder has been assumed to be having a conductivity value of a salty water (approximating the human body), about $\sigma = 5\frac{Siemen}{meter}$ at about the body temperature. The magnetic permeability of the cylinder is that of a person in the MRI machine and that is approximated to be that of free space value $\mu = \mu_0$. The frequency of the excitation current in the MRI gradient coil is taken to be $f = 3kHz$. This frequency is one of the typical values used in the actual MRI gradient switching frequency. With the above approximate values, the skin depth of the cylinder is computed as follows.

$$\delta = \frac{\sqrt{2}}{\sqrt{\omega\mu_o\sigma}} \tag{3.88}$$

$$\delta = \frac{\sqrt{2}}{\sqrt{(2\pi \times 10^3 \frac{rad}{sec})(4\pi \times 10^{-7}\frac{N}{A^2})(5\frac{S}{m})}}$$

The value of the skin depth is calculated to be $\delta = 4meter$. The skin depth is greater than the body implies that the induced current inside the body is not sufficient to perturb the B-field [39]. Substituting the value of the skin depth in equation number (3.87), and taking the value of the radial distance of the cylinder to be 20cm, the plot of the electric field inside the cylinder against the radial distance, for which we choose the axial distance to be z = 0, is shown in Fig. 3.3.

It is seen from the plot of E versus r, that the electric field is confined to the peripheral surface of the cylinder where it is more strong and can induce the eddy current.

3.6.3 Eddy Current Distribution in the Cylinder

To find the expression for the eddy current distribution amounts to multiplying the electric field expression by the conductivity σ of the cylinder. Hence the eddy current distribution will be expressed by

$$i_\phi(r,z) = -j\sigma\omega e^{\frac{r}{\delta}}\left[\sum_{i=0}^{N}\int_0^\infty D_i(k)\left(\frac{e^{\left(\frac{r}{\delta}\right)a(k)}}{\sqrt{\frac{r}{\delta}}\sqrt{2\pi a(k)}}\right)cosk(z-ih)dk\right] \tag{3.89}$$

Performing the same operations that is done for the electric field, the approximated eddy current density will be proportional to

$$i_\phi(r, z=0) \propto \sigma\vec{\omega}\frac{e^{\frac{r}{\delta}}}{\sqrt{\frac{r}{\delta}}} \tag{3.90}$$

As seen in the above equation the eddy current density is dependent on radial distance in the same manner as the electric fields but has a much greater magnitude. Using the approximated expression for the eddy current density in equation (3.90) the plot of the eddy current distribution against the radial distance is given in Fig. 3.4. And from the graph we see that the behavior of the eddy current density in the cylinder is seen to be stronger along the peripheral surface of the cylinder. Figure 3.4 is a 2D plot of the behavior of the eddy current density as a

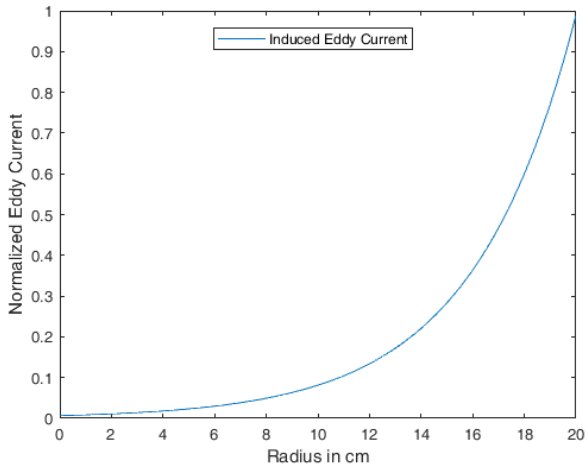

Figure 3.4: Eddy current density distribution as a function of the radius of the cylinder

function of the radius of the 3D solid cylindrical object. However, a 3D plot of the

eddy current (equation 3.90) using matlab in cylindrical coordinates yields figure 3.5. According to the color bar representing the strength of the eddy current,

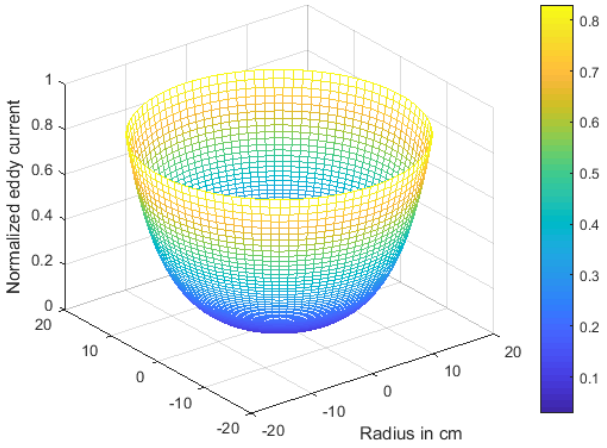

Figure 3.5: Eddy current density distribution - 3D and side view

the strongest value of the eddy current density (yellow color) is seen on the outer surface of the cylinder at the maximum value of the radius of the cylinder. Figure 3.6 is a top down view into the cylinder along the eddy current axis where the strength of the eddy current at the peripheral surface is shown again more clearly by the yellow color. the radius of the cylinder starts at the center of the cylinder. because of this piling up of the eddy current density, peripheral nerve stimulation can be induced and felt by the patient as tingling sensation and the like.

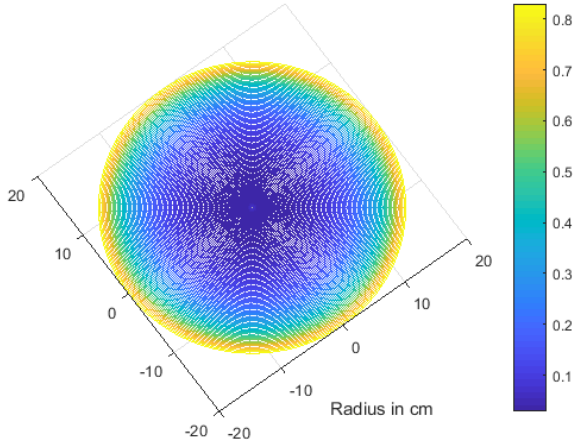

Figure 3.6: Eddy current density distribution - 3D and top-down view

CHAPTER 4
SUMMARY

In the process of imaging the current in the gradient coil is switched on and off very quickly. The increase in the switching frequency of the current in the coils helps to shorten the time of scanning and is also directly contributes to the resolution or quality of the image. Consequently quality image enables the physician to diagnose any health related problems in the body easily. Because of this, there is a need to increase the frequency of switching of the current and hence the gradient field.

The fast switching of the gradient fields caused by the quick variation of the alternating current, has a potential to induce eddy current in the skin of the patient and that may result in unwanted stimulation of the nerves and tissues. And this phenomenon is called magnetic peripheral nerve stimulation (PNS).

The objective of this study focused on the analytic determination of the induced magnetic field, electric field and the eddy current density, due to the fast switching of the current in the coils, in the chosen solid cylinder model. The coils considered are the longitudinal or Z gradient coils which are circular in shape. The solid cylinder represents the whole human body or other parts of it.

The current in the coils has a time harmonic variations. Maxwell equations were modified to suit the quasi-static situation of the problem. Using the magnetic vector potential caused by the current in the gradient coils, and taking the first order asymptotic approximation of the Modified Bessel functions, the mathematical expressions for the electric, magnetic and eddy current in the cylinder have been determined.

The plot of the electric field and the eddy current as a function of the radius of the cylinder has confirmed that the peripheral nerve stimulation actually occurs on the cylinder surface.

Increasing switching frequency is needed for better quality image and short scanning time. But as the frequency of switching increases the eddy current intensity at the surface also increases and causes PNS. PNS causes patient discomfort and can also be more dangerous for health.

The solution has the implication that the gradient coil design should focus among others, on avoiding or reducing eddy current induction and avoiding PNS. This work focused on one of the three gradient fields (the Z gradient field). In actual practice all the three are used in the process of patient scanning. However, the effect of the other two gradient fields - x and y should be a work of the future for complete understanding of the effects of all the gradient fields on PNS.

BIBLIOGRAPHY

[1] R. W. Brown, E. M. Haacke, Y.-C. N. Cheng, M. R. Thompson, and R. Venkatesan, *Magnetic resonance imaging: physical principles and sequence design*. John Wiley & Sons, 2014.

[2] S. Hidalgo-Tobon, "Theory of gradient coil design methods for magnetic resonance imaging," *Concepts in Magnetic Resonance Part A*, vol. 36, no. 4, pp. 223–242, 2010.

[3] V. Kuperman, *Magnetic resonance imaging: physical principles and applications*. Academic Press, 2000.

[4] D. Weishaupt, V. D. Köchli, and B. Marincek, *How does MRI work?: an introduction to the physics and function of magnetic resonance imaging*. Springer Science & Business Media, 2008.

[5] C. Constantinides, *Magnetic Resonance Imaging: The Basics*. CRC press, 2014.

[6] R. Aarnink and J. Overweg, "Magnetic resonance imaging, a success story for superconductivity," *Europhysics News*, vol. 43, no. 4, p. 26, 2012.

[7] N. E. Jacobsen, *NMR spectroscopy explained: simplified theory, applications and examples for organic chemistry and structural biology*. John Wiley & Sons, 2007.

[8] B. M. Dale, M. A. Brown, and R. C. Semelka, *MRI: basic principles and applications*. John Wiley & Sons, 2015.

[9] T. G. Feeman, "The mathematics of medical imaging," *Sringer,*, 2010.

[10] M. Lipton, "Totally accessible mri. 2008."

[11] D. G. Nishimura, *Principles of magnetic resonance imaging*. Stanford University, 1996.

[12] A. G. Palmer III, W. Fairbrother, J. Cavanagh, N. Skelton, and M. Rance, "Protein nmr spectroscopy: Principles and practice," 2006.

[13] H. Yan, *Signal processing for magnetic resonance imaging and spectroscopy*. CRC Press, 2002, vol. 15.

[14] E. S. Sotirchos and S. Saidha, "Oct is an alternative to mri for monitoring ms–yes," *Multiple Sclerosis Journal*, vol. 24, no. 6, pp. 701–703, 2018.

[15] D. McNeil, "Mri's strong magnets cited in accidents," *New York Times*, vol. 19, p. 2005, 2005.

[16] P. V. Prasad, *Magnetic resonance imaging: methods and biologic applications*. Springer Science & Business Media, 2006, vol. 124.

[17] G. Clarke, "The physics of clinical mr taught through images," *Medical Physics*, vol. 36, no. 5, pp. 1925–1925, 2009.

[18] A. T. Barker, R. Jalinous, and I. L. Freeston, "Non-invasive magnetic stimulation of human motor cortex," *The Lancet*, vol. 325, no. 8437, pp. 1106–1107, 1985.

[19] A. Paffi, F. Camera, F. Carducci, G. Rubino, P. Tampieri, M. Liberti, and F. Apollonio, "A computational model for real-time calculation of electric field due to transcranial magnetic stimulation in clinics," *International Journal of Antennas and Propagation*, vol. 2015, 2015.

[20] F. J. Ilmoniemi, J. Fuohonen, and J. Karhu, "Transcranial magnetic stimulation–a new tool for functional imaging," *Critical Reviews" in Biomedical Engineering*, vol. 27, no. 3-5, pp. 241–242, 1999.

[21] J. Malmivuo and R. Plonsey, *Bioelectromagnetism: principles and applications of bioelectric and biomagnetic fields*. Oxford University Press, USA, 1995.

[22] A. Thielscher and T. Kammer, "Linking physics with physiology in tms: a sphere field model to determine the cortical stimulation site in tms," *Neuroimage*, vol. 17, no. 3, pp. 1117–1118, 2002.

[23] B. J. Roth, M. Balish, A. Gorbach, and S. Sato, "How well does a three-sphere model predict positions of dipoles in a realistically shaped head?" *Electroencephalography and clinical Neurophysiology*, vol. 87, no. 4, pp. 175–184, 1993.

[24] L. G. Cohen, B. J. Roth, J. Nilsson, N. Dang, M. Panizza, S. Bandinelli, W. Friauf, and M. Hallett, "Effects of coil design on delivery of focal magnetic stimulation. technical considerations," *Electroencephalography and clinical neurophysiology*, vol. 75, no. 4, pp. 350–357, 1990.

[25] P. Tofts, "The distribution of induced currents in magnetic stimulation of the nervous system," *Physics in medicine and biology*, vol. 35, no. 8, p. 1119, 1990.

[26] S. Ueno, T. Tashiro, and K. Harada, "Localized stimulation of neural tissues in the brain by means of a paired configuration of time-varying magnetic fields," *Journal of Applied Physics*, vol. 64, no. 10, pp. 5862–5864, 1988.

[27] B. J. Roth, J. M. Saypol, M. Hallett, and L. G. Cohen, "A theoretical calculation of the electric field induced in the cortex during magnetic stimulation," *Electroencephalography and Clinical Neurophysiology/Evoked Potentials Section*, vol. 81, no. 1, pp. 47–56, 1991.

[28] V. E. Amassian, R. Q. Cracco, and P. J. Maccabee, "Focal stimulation of human cerebral cortex with the magnetic coil: a comparison with electrical stimulation," *Electroencephalography and Clinical Neurophysiology/Evoked Potentials Section*, vol. 74, no. 6, pp. 401–416, 1989.

[29] L. G. Cohen, B. J. Roth, E. M. Wassermann, H. Topka, P. Fuhr, J. Schultz, and M. Hallett, "Magnetic stimulation of the human cerebral cortex, an indicator of reorganization in motor pathways in certain pathological conditions." *Journal of Clinical Neurophysiology*, vol. 8, no. 1, pp. 56–65, 1991.

[30] B.-U. Meyer, T. Britton, H. Kloten, H. Steinmetz, and R. Benecke, "Coil placement in magnetic brain stimulation related to skull and brain anatomy," *Electroencephalography and Clinical Neurophysiology/Evoked Potentials Section*, vol. 81, no. 1, pp. 38–46, 1991.

[31] S. Ueno, T. Matsuda, and M. Fujiki, "Functional mapping of the human motor cortex obtained by focal and vectorial magnetic stimulation of the brain," *IEEE Transactions on Magnetics*, vol. 26, no. 5, pp. 1539–1544, 1990.

[32] B. J. Roth and P. J. Basser, "A model of the stimulation of a nerve fiber by electromagnetic induction," *IEEE Transactions on Biomedical Engineering*, vol. 37, no. 6, pp. 588–597, 1990.

[33] P. C. Miranda, M. Hallett, and P. J. Basser, "The electric field induced in the brain by magnetic stimulation: a 3-d finite-element analysis of the effect of tissue heterogeneity and anisotropy," *IEEE transactions on biomedical engineering*, vol. 50, no. 9, pp. 1074–1085, 2003.

[34] K. Porzig, H. Brauer, and H. Toepfer, "The electric field induced by transcranial magnetic stimulation: A comparison between analytic and fem solutions," *Serbian Journal of Electrical Engineering*, vol. 11, no. 3, pp. 403–418, 2014.

[35] G. Arfken, "Separation of variables-ordinary differential equations," *Mathematical methods for physicists*, vol. 3, pp. 448–450, 1985.

[36] H. Eaton, "Electric field induced in a spherical volume conductor from arbitrary coils: application to magnetic stimulation and meg," *Medical and Biological Engineering and Computing*, vol. 30, no. 4, pp. 433–440, 1992.

[37] J. D. Jackson, "Plane electromagnetic waves and wave propagation," *Classical electrodynamics*, pp. 273–278, 1975.

[38] S. Shen and X. Zheng, "Magnetic brain stimulation: calculation of electric field induced by arbitrary shaped coils in spherical coordinate with time variable," in *Engineering in Medicine and Biology, 2002. 24th Annual Conference and the Annual Fall Meeting of the Biomedical Engineering Society EMBS/BMES Conference, 2002. Proceedings of the Second Joint*, vol. 3. IEEE, 2002, p. 2093.

[39] R. Bowtell and R. Bowley, "Analytic calculations of the e-fields induced by time-varying magnetic fields generated by cylindrical gradient coils," *Magnetic resonance in medicine*, vol. 44, no. 5, pp. 785–786, 2000.

[40] J. A. Tegopoulos and E. E. Kriezis, *Eddy currents in linear conducting media*. North-Holland, 1985.

[41] A. Fletcher, "Guide to tables of elliptic functions," *Mathematical tables and other aids to computation*, vol. 3, no. 24, pp. 229–281, 1948.

[42] S. Okui, "Complete elliptic integrals resulting from infinite integrals of bessel functions. 11," 1974.

[43] F. F. Evans-Martin, *The nervous system*. Infobase Publishing, 2009.

[44] L. K. Forbes and S. Crozier, "On a possible mechanism for peripheral nerve stimulation during magnetic resonance imaging scans," *Physics in Medicine & Biology*, vol. 46, no. 2, p. 591, 2001.

[45] M. Davids, B. Guérin, M. Malzacher, L. R. Schad, and L. L. Wald, "Predicting magnetostimulation thresholds in the peripheral nervous system using realistic body models," *Scientific reports*, vol. 7, no. 1, p. 5316, 2017.

[46] J. Reilly, "Peripheral nerve stimulation by induced electric currents: exposure to time-varying magnetic fields," *Medical and Biological Engineering and Computing*, vol. 27, no. 2, pp. 101–103, 1989.

[47] H. N. Mayrovitz and N. Sims, "Electromagnetic linkages in soft tissue wound healing," *Wounds*, vol. 4, pp. 435–436, 2004.

[48] M. Weber and A. A. Eisen, "Magnetic stimulation of the central and peripheral nervous systems," *Muscle & nerve*, vol. 25, no. 2, pp. 160–175, 2002.

[49] K. R. Davey and C. M. Epstein, "Magnetic nerve stimulator for exciting peripheral nerves," Jul. 11 2000, uS Patent 6,086,525.

[50] W.W.Bell, *Special functions for scientists and engineers*. D.VAN NOSTRAND COMPANY,Ltd, 1968.